Geological Society of America Special Papers

Mechanisms controlling environmental change within an estuary: Corpus Christi Bay, Texas, USA

Alexander R Simms, John B Anderson, Antonio B Rodriguez, et al.

Geological Society of America Special Papers 2008;443; 121-146
doi:10.1130/2008.2443(08)

Notes

The Geological Society of America
Special Paper 443
2008

Mechanisms controlling environmental change within an estuary: Corpus Christi Bay, Texas, USA

Alexander R. Simms
Boone Pickens School of Geology, Oklahoma State University, 105 NRC, Stillwater, Oklahoma 74074, USA

John B. Anderson
Department of Earth Science, Rice University, 6100 Main Street, MS 126, Houston, Texas 77005, USA

Antonio B. Rodriguez
Institute of Marine Sciences, University of North Carolina at Chapel Hill, 3431 Arendell Street, Morehead City, North Carolina 28557, USA

Marco Taviani
Instituto di Scienze Marine, Consiglio Nazionale delle Ricerche, via Gobetti 101, Bologna, 40129, Italy

ABSTRACT

Over 400 km of high-resolution seismic data and 53 sediment cores up to 30 m in length were collected from Corpus Christi Bay along the central Texas coast in order to study the impact of sea-level and climate change on coastal environments over the last 10 k.y. Although coastal environments experienced a general landward migration as relative sea level rose over the last 10 k.y., this retreat was punctuated by three, possibly four, major flooding events. These flooding events are marked by abrupt changes in lithologic and seismic facies interpreted to represent rapid landward shifts of bay environments. Such changes include the back stepping of bayhead deltas, tidal deltas, oyster reefs, and other bay environments. Flooding events occurred at 8.0, 4.8, 2.6 ka, and possibly at 9.6 ka, and lasted only a few hundred years. The 9.6 ka flooding surface represents the initial drowning of the ancestral Nueces River valley and may or may not have been rapid in nature. The flooding surface that formed around 8.0 ka is interpreted to record either an increase in the rate of relative sea-level rise or the flooding of relict fluvial terraces that formed by the Nueces River during the stepped fall in sea level since marine isotope stage (MIS) 5e (120 ka). The 4.8 ka flooding event is thought to have formed as a result of either a climatic change during the mid-Holocene, characterized by warmer and drier conditions compared to present, and/or the flooding of another fluvial terrace. The most recent flooding event (2.6 ka) is thought to have resulted from a decrease in sediment delivery to the bay associated with a return to more mesic conditions similar to those of the present climatic regime.

Keywords: Holocene, Gulf of Mexico, sea level, incised valley, coastal evolution.

Simms, A.R., Anderson, J.B., Rodriguez, A.B., and Taviani, M., 2008, Mechanisms controlling environmental change within an estuary: Corpus Christi Bay, Texas, USA, *in* Anderson, J.B., and Rodriguez, A.B., eds., Response of Upper Gulf Coast Estuaries to Holocene Climate Change and Sea-Level Rise: Geological Society of America Special Paper 443, p. 121–146, doi: 10.1130/2008.2443(08).

INTRODUCTION

With the recent attention given to global warming, many studies have focused on the incipient increase in the rate of sea-level rise and its potential impact on coastal systems. However, coastal systems are dynamic and sensitive not only to changes in the rate of sea-level rise but also to other factors, such as climate change and the flooding of relict topography. The purpose of this study is to document the changes that occurred within the Corpus Christi Bay system over the last 10 k.y., a time period that is known to have experienced varying rates of sea-level rise and climatic changes. From this work, we document the effects of these and other agents of coastal change, such as the flooding of relict topography.

Corpus Christi Bay was chosen as a study site due to its location within the flooded ancestral valley (incised valley) of the Nueces River (Brown et al., 1976; Wright, 1980; Shideler, 1986; Durbin et al., 1997; Morton and Kindinger, 1998; Simms et al., 2006b). Incised valleys often preserve the most complete records of coastal change due to their high preservation potential in light of transgressive ravinement (Belknap and Kraft, 1981, 1985). In addition, most coastal studies have focused on systems that lie in humid or subhumid climate zones (Belknap and Kraft, 1985; Bratton et al., 2003; Baeteman et al., 2002), while this study documents the changes that have occurred within a semiarid climatic setting.

STUDY AREA

Corpus Christi Bay lies along the central Texas coast of the northwestern Gulf of Mexico (Fig. 1). This portion of the Gulf of Mexico represents a passive margin with a very gentle coastal plain. The average coastal-plain gradient is 0.28 m/km, and the average continental-shelf gradient is 3 m/km, calculated from the location of the 200 m contour. The subsidence rates along the central Texas coast are very low, averaging less than 0.05 mm/yr (Paine, 1993).

Corpus Christi Bay has an average water depth of between 3 and 4 m (Fig. 1B). Nueces Bay, a shallower (average 1 m depth) tributary bay of Corpus Christi Bay, occupies the landward-most reaches of the flooded Nueces River. It is separated from Corpus Christi Bay by Rincon and Indian Points. Corpus Christi Bay is connected to the Gulf of Mexico through two ephemeral inlets: Aransas Pass and the historically active Corpus Christi Pass (Morton and McGowen, 1980; Fig. 1). The bay lies within a subhumid to semiarid climate zone (Thornthwaite, 1948) and receives 68–89 cm/yr of precipitation at the present coastline, with a decrease in precipitation with greater distances from the coast (Carr, 1967; White et al., 1983). Evaporation within the area exceeds precipitation by 16–20 cm/yr (White et al., 1983). Winds are predominately from the southeast (Lohse, 1956), although winter storms bring winds from the north (Morton and McGowen, 1980; Shideler, 1984). Hurricanes have undoubtedly played an important role in the evolution of the coast, especially in the lower bay area (Snedden et al., 1988). They are an important agent in the delivery of sand to the estuarine system via overwash and breaching of the barrier-island system, as well as the flooding of rivers and streams flowing into the bay. Over historic times, the probability of their occurrence is ~7% in any one year (Simpson and Lawrence, 1971; White et al., 1983), but the past frequency of hurricanes throughout the Holocene is unknown. The current astronomical tidal range of the bay is <0.3 m (Marmer, 1954; Shideler, 1984).

The Nueces River is the principal supplier of freshwater and sediment (Yeager et al., 2006), delivering 6.3×10^8 m^3 yr^{-1} of freshwater (Henley and Rauschuber, 1981; Mannino and Montagna, 1996) and 750,000 tons yr^{-1} of sediment to the bay (predam; Shepard, 1953). The climate along the length of the Nueces River is similar to that of Corpus Christi Bay—generally a semiarid climate with slightly drier conditions in its upper reaches, which receive just over 50 cm/yr of precipitation (Carr, 1967).

Sea Level

Sea level along the northwestern Gulf Coast has risen between 90 and 120 m over the last 20 k.y. (Fig. 2; Shepard and Suess, 1956; Curray, 1960; McFarlan, 1961; Nelson and Bray, 1970; Törnqvist et al., 2004a; Simms et al., 2007). Two camps have risen within the coastal and shelf community as to whether the postglacial rise was continuous (Shepard and Suess, 1956; McFarlan, 1961; Coleman and Smith, 1964; Törnqvist et al., 2004a) or episodic, with rapid increases in the rate of sea-level rise around 15, 11, 9, 8.2, 7, 2.5, and 1.2 ka (Rehkemper, 1969; Nelson and Bray, 1970; Penland et al., 1988; Thomas and Anderson, 1994; Törnqvist et al., 2004b). Recent work in the Trinity incised valley suggests that some of these sea-level events might have been the result of other mechanisms, such as the flooding of flat antecedent topography (Rodriguez et al., 2005). Morton et al. (2000) and Blum et al. (2001, 2002) have made arguments for a mid-Holocene highstand and fall in sea level since 6.5 ka.

Coral-based sea-level records indicate two rapid increases in the rate of sea-level rise occurring at 14.5 ka (meltwater pulse [MWP] 1-A) and 11.3 ka (MWP 1-B; Fairbanks, 1989; Chappell and Polach, 1991; Bard et al., 1996). Evidence for a much smaller climatic event with a possible small "eustatic" rise in sea level around 8.2 ka has been presented by Alley et al. (1997), and within the Gulf of Mexico, by Törnqvist et al. (2004b). Given the uncertainty in dating, the timing of the first two Gulf of Mexico events (15 ka and 11 ka) could correspond to MWP 1-A and 1-B, but, with the exception of the 8.2 ka event, the latter five events have no known "eustatic" equivalents. However, the resolution of these coral-based "eustatic" records is only 5 m (Lighty et al., 1982), and lower-amplitude events could have occurred.

Work from northwest Europe (Morner, 1980; Streif, 2004), the Atlantic Coast of the United States (Fletcher et al., 1993), and the Gulf Coast (Suku and Pizzuto, 1995; Donoghue and White, 1995; Walker et al., 1995; Froede, 2002; Stapor and Stone, 2004) suggests the presence of higher-order oscillations in sea level

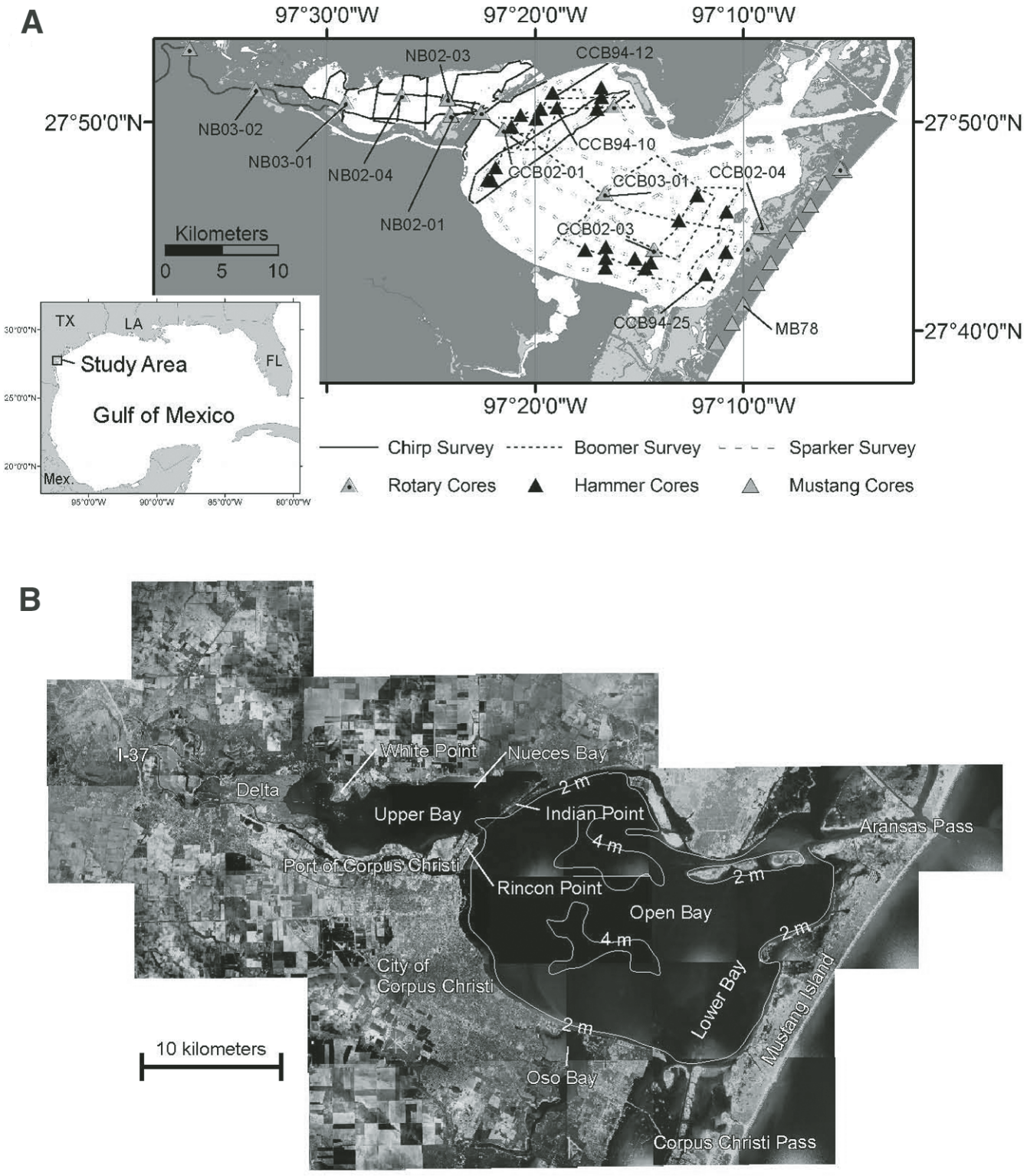

Figure 1. (A) Study area and data map. White areas represent water, dark gray areas represent land, and light gray areas represent intertidal areas. (B) Aerial photograph of Corpus Christi Bay showing the locations of major geographic features and bathymetric contours for the bay (data courtesy of the Texas General Land Office).

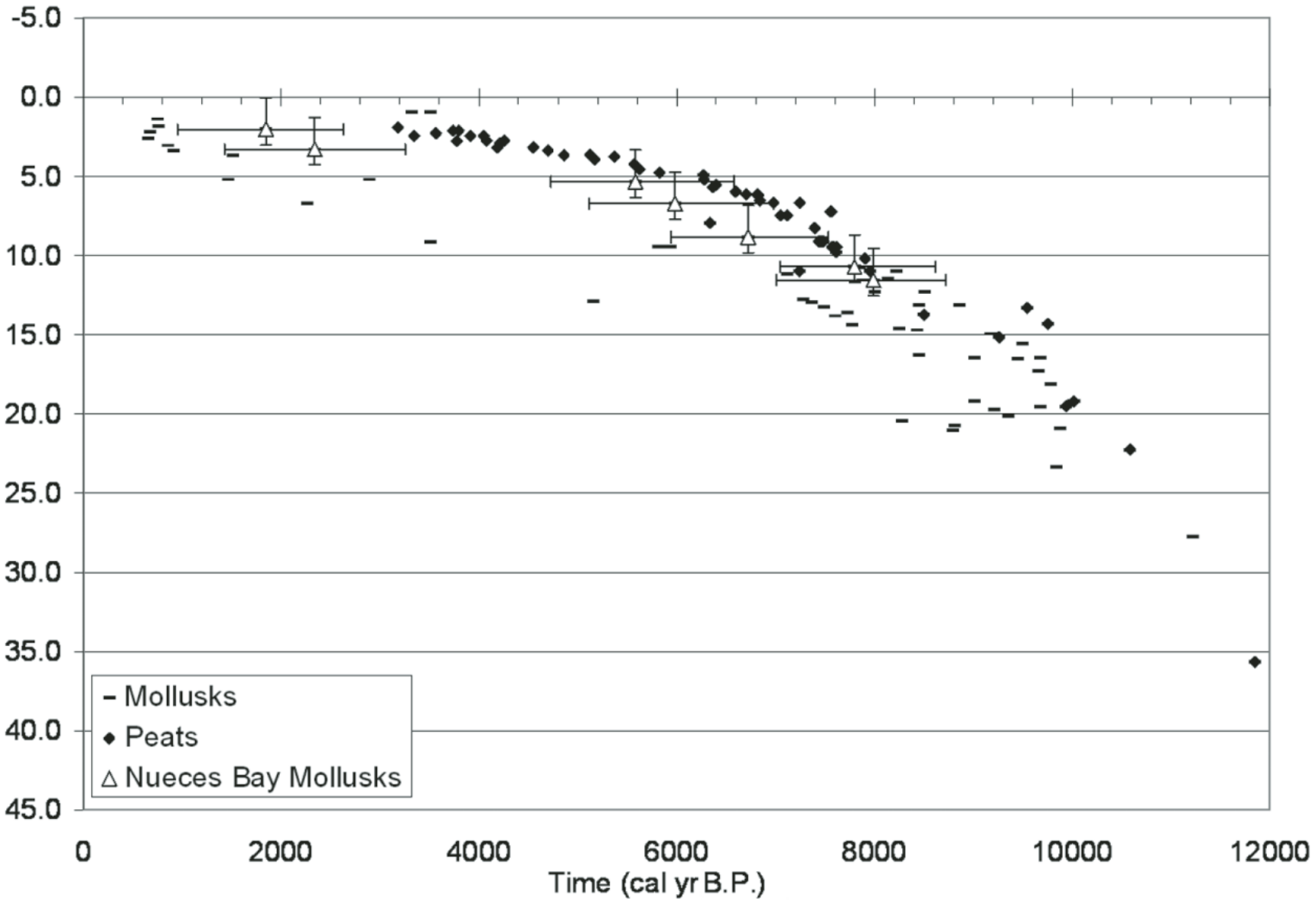

Figure 2. Sea-level indices from across the coastal areas of the northwestern Gulf of Mexico. Data come from Shepard and Moore (1955), Curray (1960), Rehkemper (1969), Nelson and Bray (1970), Rodriguez et al. (2004), Törnqvist et al. (2004a), and this study. Estuarine deposits were obtained from either wood fragments or mollusk shells. Peats were interpreted by each of the respective authors to represent basal peats. Nueces Bay dates were obtained from mollusk shells (this study).

with amplitudes less than 1 m over the last 6 k.y. We were unable to test the validity of these higher-amplitude oscillations within the study area since oscillations of this magnitude are below the resolution of this data set.

In addition, other effects such as glacio-hydro-isostasy and subsidence will cause differences between the relative sea-level history of the Gulf of Mexico and the study area and sea-level records from other locations globally (Lambeck and Chappell, 2001; Simms et al., 2007). Given the Gulf of Mexico's intermediate-field location (Peltier et al., 1978), the amplitudes but not direction of sea-level history could be different from the "eustatic" sea-level curve. For the purposes of this study, we use a compilation of relative sea-level curves based on several data sets from the Gulf of Mexico to bracket the sea-level history experienced by the Corpus Christi Bay system (Curray, 1960; Nelson and Bray, 1970; Rodriguez et al., 2004; Törnqvist et al., 2004a). Each of these sea-level curves suggest a continual slow rise in relative sea level since ca. 8 ka and decreases in the rate of relative sea-level rise at 5.5 and 3.2 ka (Fig. 2). This behavior has also been documented along the Atlantic Coast of the United States (van de Plassche et al., 1989; van de Plassche, 1990).

METHODS AND DATA

Data

Over 400 km of high-resolution seismic data and 53 sediment cores were used in this study (Fig. 1). In addition, over 90 core descriptions from the U.S. Army Corp of Engineers and the Texas Department of Transportation were used to help supplement this data set. Three seismic data sets were used, each from a different source: a minisparker survey conducted by the U.S. Geological Survey in 1978, a boomer survey conducted by Rice University in 1994, and another boomer survey conducted by the U.S. Geological Survey in 1996. The only processing of seismic lines was simple band-pass filters and automatic gain control. Three methods of coring were used, 25 hammer cores up to 4 m in length taken on the R/V *Lone Star*, 11 rotary cores up to 22 m in length, and 8 vibracores up to 5 m in length taken on the R/V *Trinity*. Nine push cores up to 30 m in length taken by the U.S. Geological Survey on Mustang Island were also used (Simms et al., 2006a). In addition to lithological data, 10 of the 11 rotary core sites were logged using a Mount Sopris 2PGA-1000 gamma logger. Gamma logs helped to constrain the lithology of sections where core sampling was incomplete or limited. This was most helpful in delineating the exact thicknesses of very sandy intervals with limited core recovery. Lithological data with radiocarbon ages were tied to seismic data to construct paleogeographic maps of the bay for the past 10 k.y.

Lithology

Grain-size analyses using laser diffractometry (Malvern Sizemaster 2000) were conducted at approximately every 25 cm within the cores. A refractive index of 1.544 was used following the "pipette" method of Sperazza et al. (2004). In addition to grain-size analyses, the samples were washed, and the sand-sized fraction (>63 um) was analyzed. Coarse-fraction analysis (relative percentage of sand, organic material, forams, and shell material) was developed for distinguishing marginal-marine and shallow-marine environments along the central Texas shelf and coast by Shepard and Moore (1954, 1955) and found to be of great use by Rehkemper (1969) in environmental interpretation within Galveston Bay in east Texas. A modified version of this method was used to help distinguish the 13 lithological units described in this study. Over 500 samples of the >63 µm fraction from 25 cores were randomly selected and sorted (without knowledge of their origin). In addition to the relative importance of major constituents within the >63 µm component, sorting and lithology were also used to help subdivide the samples. The macrofauna (mainly mollusks) and sedimentary structures (identified as homogeneous, or structureless, mottled, irregular bedding, or regular bedding; Moore and Scruton, 1957) within each core were also examined to help define and interpret the lithological facies.

Seismic Velocity

Seismic velocities were calculated based on the assumption that the most drastic seismic facies change came at the Pleistocene-Holocene contact or a distinct mud-sand contact. Six such contacts in cores and seismic profiles were found, resulting in calculated velocities of 1636 m/s, 1559 m/s, 1500 m/s, 1557 m/s, 1548 m/s, and 1680 m/s. The mean of these values results in an average seismic velocity of 1580 m/s. This number falls within the values obtained in a check-shot survey conducted on similar sediments offshore (Abdulah, 1995) and to other seismic studies of late Pleistocene–Holocene sediments of the Gulf Coast and shelf (Shideler, 1986; Sydow and Roberts, 1994; Anderson et al., 2004; Bartek et al., 2004). Although variations are expected from the averaged value, a remarkably good fit was found between lithologic and seismic facies boundaries.

Chronostratigraphy

Over 50 radiocarbon dates were obtained from mollusk and wood fragments (Table 1). When possible, only articulated mollusks were used. The samples were sent to the National Ocean Sciences Accelerator Mass Spectrometry Facility (NOSAMS) and Beta Analytic for dating and corrected at each laboratory for the ratio of $^{13}C/^{12}C$. Dates were remarkably consistent with depth in all of the cores taken within Corpus Christi Bay. Some inconsistencies in the age with respect to depth were found in cores obtained from the lower bay environment.

Carbon reservoir effects on ^{14}C dating are known to occur within the estuaries of the Gulf Coast (Aten, 1983) and within fluvial and marine systems around the world (Raymond and Bauer, 2001). To test for a possible carbon reservoir within the deposits from Corpus Christi Bay, two dates were obtained from an articulated barnacle growing on a wood fragment found within a muddy unit in core NB02-04 at a depth of 15.0 m. The barnacle

TABLE 1. RADIOCARBON DATES COLLECTED FOR THIS STUDY

Core	Depth (m)	Depth (m bsl)	Species	Uncorrected age (yr)	Error (±yr)	Reservoir (yr)	Reservoir error (yr)	Calibrated age (yr B.P.)	2σ (yr)
Corpus Christi Bay									
CCB02-01	3.47	8.04	*Nuculana concentrica*†	2310	40	760	380	1500	830
CCB02-01	4.78	9.35	*Abra ovalis*†	2530	45	760	380	1740	970
CCB02-01	6.22	10.79	*Nuculana concentrica*‡	3290	35	760	380	2610	950
CCB02-01	8.12	12.69	*Mulinia lateralis*†	4550	40	760	380	4200	1090
CCB02-01	9.47	14.04	*Nuculana concentrica*†	6270	40	760	380	6310	940
CCB02-01	10.94	15.51	*Nuculana concentrica*	7520	130	760	380	7620	870
CCB02-01	12.6	17.17	*Mulinia lateralis*	7750	50	760	380	7850	820
CCB02-01	15.62	20.19	*Mulinia lateralis*	8750	40	760	380	8900	890
CCB02-01	17.01	21.58	*Brachidontes exustus*	9360	55	760	380	9650	1040
CCB02-01	20.29	24.86	Wood fragment	5690	30	0	0	6470	80
CCB02-03	4.7	10.18	*Mulinia lateralis*	4480	40	760	380	4110	1160
CCB02-03	8.23	13.71	*Mulinia lateralis*	4280	50	760	380	3850	990
CCB02-03	12.22	17.7	*Nuculana concentrica*	1730	35	760	380	930	930
CCB02-04	5.6	7.73	*Anomalocardia cuneimeris*	2130	30	0	0	2110	150
CCB02-04	7.01	9.14	*Anomalocardia cuneimeris*	2130	35	0	0	2110	150
CCB02-04	11.82	13.95	*Mulinia lateralis*	4620	40	0	0	5420	70
CCB02-04	14.85	16.98	*Anomalocardia cuneimeris*	2060	35	0	0	2020	95
CCB03-01	3.52	7.85	*M. lateralus* or *R. flexuosa*‡	2390	30	760	380	1585	850
CCB03-01	6.66	10.99	*Mulinia lateralis*†	4470	35	760	380	4100	1160
CCB03-01	7.64	11.97	*Rangia flexuosa*‡	5010	30	760	380	4800	1070
CCB03-01	12.71	17.04	Unknown fragment	6520	55	760	380	6590	840
CCB03-01	13.48	17.81	*M. campechiensis texana*	6780	45	760	380	6870	860
CCB03-01	14.73	19.06	*M. campechiensis texana*	7500	45	760	380	7600	800
CCB03-01	15.44	19.77	*Nuculana concentrica*†	7890	60	760	380	7980	970
CCB03-01	16.29	20.62	*Abra aequalis*†	8050	40	760	380	8140	860
CCB03-01	17.25	21.58	*Nuculana concentrica*†	8470	40	760	380	8590	880
CCB03-01	20.09	24.42	*Nuculana concentrica*?	9240	65	760	380	9480	1000
Nueces Bay									
NB02-01V	0.48	2.92	*Mulinia lateralis*†	730	45	760	380	Modern	
NB02-01 V	1.66	4.1	*Crassostrea virginica*†	3260	60	760	380	2570	950
NB02-01	5.18	7.62	*Nuculana concentrica*	4710	55	760	380	4400	1050
NB02-01	7.31	9.75	*Nuculana concentrica*	4880	60	760	380	4630	990
NB02-01	10.28	12.72	*Nuculana concentrica*†	7060	60	760	380	7140	820
NB02-01	12.07	14.51	Barnacle†	8000	65	760	380	8090	910
NB02-03	5.4	6.62	*Nuculana concentrica*†	4420	55	3660	380	4030	1030
NB02-03	7.13	8.35	*Abra ovalis*‡	6420	60	5660	380	6480	840
NB02-04	15.03	16.25	Barnacle†	8430	45				
NB02-04	15.04	16.25	Wood	7670	45	0	0	8484	100
NB03-01	1.2	2.02	*Mulinia lateralis*†	2630	45	1870	380	1850	900
NB03-01	2.45	3.27	*Mulinia lateralis*‡	3060	45	2300	380	2340	920
NB03-01	4.5	5.32	*Mulinia lateralis*‡	5640	60	4880	380	5580	1000
NB03-01	5.9	6.72	*Macoma mitchelli*†	5980	60	5220	380	5980	1000
NB03-01	8	8.82	*Nuculana acuta*	6640	50	5880	380	6720	830
NB03-01	9.86	10.68	*Rangia flexuosa*†	7700	70	6940	380	7800	800
NB03-01	10.71	11.53	*Nuculana concentrica*†	7900	100	7140	380	7990	980
NB03-02	0.99	0.99	Plant/Wood	30	–33.2	0	0	30	33
NB03-02	3.67	3.67	Plant/Wood	35	–60.5	0	0	35	60
NB03-02	3.96	3.96	*Macoma mitchelli*‡	5160	40	760	380	4990	1010
NB03-02	4.77	4.77	*Macoma constricta*†	2990	30	760	380	2250	910
Mustang Island									
MB78	7.5	6.5	*Anadara* sp.‡	5440	40	0	0	6240	65
MB78	13.5	12.5	*Donax* sp.‡	4500	35	0	0	5170	130
MB78	16.7	15.7	*Mulinia lateralis*‡	5700	30	0	0	6480	80
MB78	20.8	19.8	*Donax* sp.‡	5730	30	0	0	6520	110

†Articulated.
‡Valve.

and wood fragment were dated separately. The date obtained from the barnacle was 760 yr older than that obtained from the wood fragment. The difference in age between the barnacle and wood fragment is consistent with a radiocarbon reservoir—the mollusk yielded an older age in comparison with the plant fragment. Although variability in the radiocarbon reservoir probably exists over time and with species, this value was assumed to represent the reservoir correction for mollusks within Corpus Christi Bay. To account for variations in the reservoir, we used a reservoir uncertainty of 50% when calibrating the ages. A reservoir value of 760 yr falls within the range of other reservoir corrections found in other estuaries of the Gulf Coast (Aten, 1983) and brings near-surface dates obtained in this study to modern values. This radiocarbon reservoir was applied to all dates obtained from mollusks that are known to inhabit estuaries. Dates obtained from whole valves of *Donax* sp. were assumed not to be affected by a radiocarbon reservoir due to their habitation of the high-energy surf zone adjacent to the open ocean, which is thought to have a rapid exchange of ^{14}C with the atmosphere (Stuiver and Braziunas, 1993). After correcting for the reservoir effect where appropriate, carbon dates were calibrated to calendar years using the terrestrial Northern Hemisphere curve of the Calib 4.4 program (Stuiver and Braziunas, 1993; Stuiver et al., 1998). All dates discussed in this paper are calibrated, corrected for ^{13}C content, corrected for reservoir effects, and given in calendar yr B.P. When dates from other sources are given, the same procedure was followed.

RESULTS AND INTERPRETATION

Lithology

Apart from Pleistocene deposits, four broad types of facies were distinguished within the Holocene deposits: mud facies, sand facies, shell hash facies, and oyster facies. Of these four facies, mud is the most variable and widespread. All mud facies contain less than 20% sand and record values of >20 counts per second (cps) in gamma logs. All the sand facies consist of greater than 20% sand, most around 50% sand, and a gamma log value <20 cps. A brief summary of each lithofacies is given in Table 2.

Mud Facies (MF)

MF1. Mud facies 1 is a light gray structureless mud with an average sand content of 10% (Fig. 3A). Plant fragments are not present in appreciable amounts. The sand component is extremely well-sorted, quartz-rich (>95%), and fine to very fine in size. The facies contains sparse shells, and forams constitute, on average, a larger portion of the coarse fraction than shell material. Of the few shells present, the populations are dominantly *Nuculana acuta*, *N. concentrica*, and *Mulinia lateralis*. This facies occurs within cores from depths down to 20 m below sea level (bsl) from two general areas: middle Nueces Bay updip from Rincon and Indian Point and middle Corpus Christi Bay. Samples from the middle of Corpus Christi Bay contained an occasional *Anomia simplex*, *Ostrea equestris*, *Mercenaria campechiensis texana*, *Abra aequalis*, or *Dentalium texasianum*, while the samples from Nueces Bay contained an occasional juvenile *Rangia flexuosa* and *Macoma mitchelli*. Ostracodes and possible fecal pellets were also present within the facies within Nueces Bay. Mud facies 1 is interpreted to represent an open-bay deposit and reflects deposition that is well removed from any significant sources of sand (i.e., bayhead delta or bay margins). The open-bay environment in Corpus Christi Bay is more saline than within Nueces Bay, indicating an open-bay environment located distal from the bayhead delta within Corpus Christi Bay and restricted or interdistributary bay located behind the main distributaries of the active bayhead delta in Nueces Bay.

MF2. Mud facies 2 is generally darker gray and contains more sand and shell material than MF1 (Fig. 3B). Mud facies 2 lacks sedimentary structures. Of its coarse fraction, shells are the most abundant constituent. Forams are less abundant than sand grains. The mineralogic fraction is an extremely well-sorted, quartz-rich (>95%), fine to very fine sand. The shells within this facies are often concentrated in discrete layers, presumably storm deposits. The most abundant shells within this facies are *Nuculana acuta*, *N. concentrica*, *Mulinia lateralis*, *Mercenaria campechiensis texana*, *Abra aequalis*, *Chione cancellata*, and *Dentalium texasianum*. This facies is present in the upper 3 m of almost every core collected in Corpus Christi Bay. It is never found below a depth of 5 m. MF2 is interpreted to be deposits that accumulated in an open-bay setting analogous to the environmental conditions within the present Corpus Christi Bay.

MF3. Mud facies 3 consists of a laminated gray mud with sparse to no shells (Fig. 3E). Mineralogic sand is the most abundant coarse fraction component (>90%). Forams, shells, and plant fragments are present but in very small quantities. Generally, the mineralogic sand component is well-sorted, fine to very fine in size, and quartz-rich. Shells include juvenile *Rangia flexuosa* and *Macoma mitchelli*. This lithofacies is interpreted to represent a prodelta environment.

MF4. Mud facies 4 consists of an irregular (nonplanar, discontinuous, or wavy) bedded gray mud (Fig. 3C). Mineralogic sand is the dominant coarse fraction, and forams and shells constitute only a minor component. The mineralogic sand fraction is generally poorly sorted and is mostly fine-grained; however, medium lithic grains also occur. Organic material is present within this facies, often in discrete irregular layers. Shells include juvenile *Rangia flexuosa*, *Mulinia lateralis*, and an occasional oyster (*Crassostrea virginica* or *Ostrea equestris*). This lithofacies is interpreted to represent upper-bay deposits.

Sand Facies (SF)

SF1. Sand facies 1 is actually a sandy mud. A large proportion of the sand component is found within sand-filled burrows or root casts (Fig. 3D). The sand fraction is moderately sorted and composed dominantly of quartz. Shells and forams are rare to absent. Plant material is an abundant constituent of this facies.

TABLE 2. SUMMARY OF LITHOFACIES DESCRIBED IN THIS STUDY, THEIR EQUIVALENT SEISMIC FACIES, AND ENVIRONMENTAL INTERPRETATION

Lithofacies	Brief description	Seismic facies	Interpreted depositional environment
MF1	Structureless gray mud, <10% sand, few shells	F1, F4	Open bay
MF2	Sandy gray mud, shell layers	F1	Open bay
MF3	Well-laminated gray mud, very little shell material	F2	Prodelta
MF4	Irregularly bedded gray sandy mud	F2	Upper bay
SF1	Sandy organic-rich mud	F2	Delta plain
SF2	Poorly sorted, medium sand, lithic-rich	F2, F6	Mouth bar
SF3	Muddy sand/sandy mud, mixed brackish-marine fauna	F5	Lower bay
SF4	Clean, very-well-sorted quartz sand	NA	Barrier island
SF5	Structureless, light gray sandy mud	F2, F5	Delta front
SF6	Interbedded fine sand and mud	F5	Distal flood-tidal delta
ShF1	Well-sorted shell hash, dominantly oyster fragments	Cuspate seismic features	Interbay tidal inlet
ShF2	Sandy shell hash, mixed marine/brackish fauna	NA	Tidal inlet
OF1	Muddy oyster shells	F3	Oyster reef

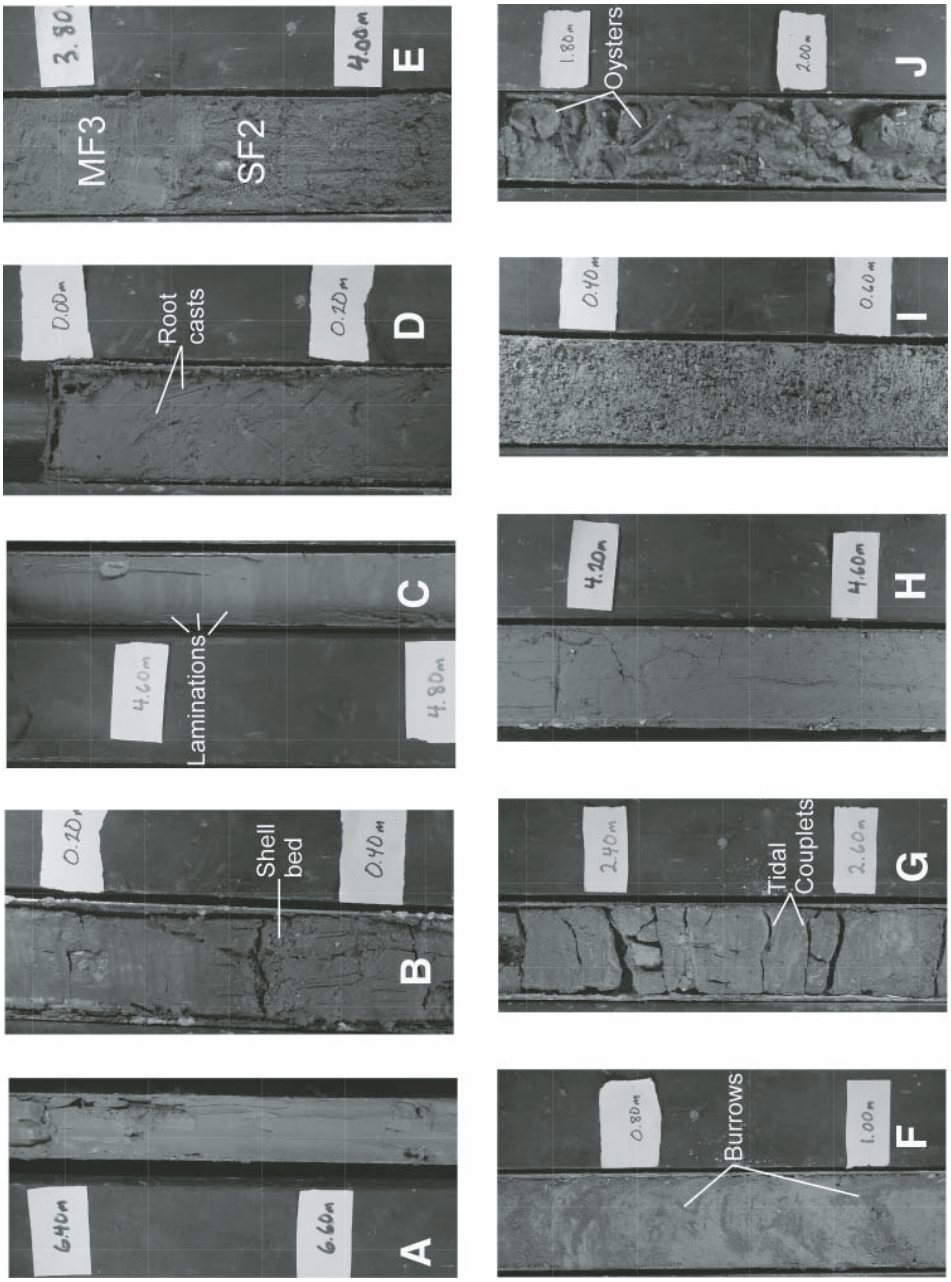

Figure 3. Examples of selected lithofacies from cores taken within Corpus Christi Bay. (A) MF1 from core CCB03-01, (B) MF2 from core CCB94-10, (C) MF4 from core NB03-01, (D) SF1 from core NB03-02, (E) SF2 below MF3 from core NB03-02, (F) SF3 from core CCB94-25, (G) SF5 from core CCB94-3, (H) SF6 from core NB02-01VC, (I) ShF1 from core NB02-03VC, and (J) OF1 from core NB02-03 VC. The vertical scale for each photograph is 10 cm. MF—mud facies; SF—sand facies; Shf—shell-hash facies.

SF1 is interpreted to represent delta-plain deposits of the Nueces bayhead delta.

SF2. Sand facies 2 is a structureless, muddy, poorly sorted, medium sand (Fig. 3E). The mineralogic sand component is relatively lithic-rich (<75% quartz). It has abundant to no shell and plant material. Occasionally, this facies has abundant oyster-reef fauna (*Crassostrea virginica*, *Ostrea equestris*, *Brachidontes* sp.). Other fauna include *Macoma mitchelli*, *Tagelus plebeius*, *Rangia flexuosa*, and *Turbonilla* sp. It is interpreted to represent a mouth bar within a bayhead delta.

SF3. Sand facies 3 is a muddy sand/sandy mud. The mineralogic sand component is fine, well-sorted, and quartz-rich (>95%). It has few to abundant shells. The fauna, being mixed in origin with both brackish- and open-marine species, is the most diagnostic characteristic. *Anomalocardia auberiaus*, *Polymesoda maritima*, *Crassinella lunulata*, *Lucina amiantus*, *Lucina multilineata*, *Donax* sp., *Cerithium lutosum*, *Anadara transversa*, *Ostrea equestris*, *Mulinia lateralis*, and *Chione cancellata* are found within this facies. Occasionally, the facies shows irregular bedding, mottling, or burrows (Fig. 3F). In longer cores, it lacks sedimentary structures. It is interpreted to represent lower-bay (washover) deposits.

SF4. Sand facies 4 is a clean, quartz-rich, very well-sorted, fine to very fine sand. It has a uniform grain size of 2.6–2.7 phi

and contains less than 10% mud. No sedimentary structures were preserved within the cores that sampled SF4. Shell and organic material are occasionally found. When present, fauna are dominantly *Donax* sp. and *Anomalocardia cuneimeris*. This facies is interpreted as undifferentiated barrier-island deposits. Distinction between barrier-flat, beach, and eolian deposits was attempted (Simms et al., 2006a) but not important to this study.

SF5. Sand facies 5 is similar to sand facies 1. However, sand facies 5 is generally lighter gray in color and contains less sand and more shell material (Fig. 3H). In addition, root casts and burrows are absent, and no other sedimentary structures are found. The fauna within this facies include *Turbonilla* sp., *Nuculana acuta*, *Nuculana concentrica*, and *Dentalium texasianum*. This facies is interpreted to be delta-front deposits based on these criteria and its association with clinoforms in seismic profiles.

SF6. Sand facies 6 is an interbedded fine sand and mud (tidal couplets; Fig. 3G). The sand component is fine to very fine in size. Very few shells are found directly within this facies; however, this facies is always found in association with SF3 and its accompanying fauna. This deposit is interpreted to be a distal flood-tidal delta facies.

Shell-Hash Facies (ShF)

ShF1. This shell-hash facies is a structureless well-sorted shell hash (Fig. 3I). It is composed almost exclusively of millimeter-sized oyster fragments (*Crassostrea virginica* and possibly *Ostrea equestris*) and associated mussels (*Brachidontes* sp.). This facies is only found in the top of a core near Rincon and Indian Points (Fig. 1), which separate Corpus Christi and Nueces Bays. It is interpreted to be a modern interbay tidal-inlet deposit. Wind tides rather than tidal circulation are thought to have been the dominant process operating in this environment due to the relatively low tidal range and depth of Nueces Bay and the strong winds that persist within the bay, which is aligned parallel to the dominant wind direction (Shideler, 1984).

ShF2. Shell-hash facies 2 is a structureless, poorly sorted sandy shell hash. Occasional whole valves can be found. The fauna is more diverse than ShF1, containing both estuarine and shallow-marine fauna. Fragments of *Nuculana acuta*, *Nuculana concentrica*, *Lucina multilineata*, *Lucina amiantus*, and *Chione cancellata* are all present. This deposit is interpreted to be a proximal tidal-inlet facies.

Oyster Facies (OF)

OF1. Oyster facies 1 consists of articulated oysters (mostly *Crassostrea virginica* with an occasional *Ostrea equestris*) within a muddy matrix (Fig. 3J). Other fauna include *Brachidontes* sp., *Chione cancellata*, *Nuculana acuta*, and *Anomia simplex*.

Pleistocene

Pl. Undifferentiated Pleistocene deposits were sampled in a few locations. Generally, they consist of a very stiff gray or tan mottled mud with calcareous nodules and a gamma log value >60 cps. A mollusk shell taken from the stiff mud unit beneath Mustang Island yielded a radiocarbon dead result (Simms et al., 2006a). Beneath Mustang Island, a sand unit was also interpreted to be Pleistocene in age. It is thought to represent alluvium associated with buried fluvial "Deweyville" terrace deposits based on its more lithic and coarse-grained nature, yellow color, and stratigraphic position (Simms et al., 2006a).

Seismic Facies

Six seismic facies were found above the interpreted Pleistocene-Holocene contact. These are illustrated in Figure 4.

F1

Seismic facies 1 consists of horizontal, parallel, medium-amplitude continuous reflectors (Fig. 4). Seismic facies 1 often contains large mounds of seismic facies 3. In terms of lithology, seismic facies 1 corresponds with MF1 and MF2. F1 is interpreted as open-bay deposits.

F2

Seismic facies 2 is composed of nearly parallel, high-amplitude, nearly continuous reflectors (Fig. 4). F2 has more wavy and irregular reflectors relative to F1 and often contains smaller mounds of F3. When sampled, this seismic facies corresponds with lithological facies SF1, SF2, SF5, MF3, MF4, and, in two cases, MF1. F2 is interpreted to represent an upper-bay environment.

F3

Seismic facies 3 is composed of mounded, high-amplitude reflectors (Fig. 4). Continuous reflectors on either side onlap these mounds. This seismic facies was sampled by core NB02-01 VC, which sampled lithological facies OF1. In addition, cores sampling the surrounding seismic facies F1, F2, and F4, when near mounds of F3, often contained fragments of oyster shells (*Crassostrea virginica* and *Ostrea equestris*). F3 is interpreted as oyster reefs.

F4

Seismic facies 4 is nearly acoustically transparent (Fig. 4). Faint continuous, parallel reflectors occasionally occur. In terms of lithology, F4 corresponds with MF1. In addition, samples of MF1 within F4 always contain very little sand (<5%). This seismic facies is interpreted to represent open-bay deposits.

F5

Seismic facies 5 is composed of sigmoid-oblique to oblique-parallel reflectors (Fig. 4). Cores that sampled F5 contain lithological facies SF3 or SF5. This seismic facies is interpreted to represent deltaic deposits (either bayhead or tidal deltas).

F6

Seismic facies 6 is chaotic in nature (Fig. 4). The cores that sampled F6 contain lithological facies SF2. This seismic unit is

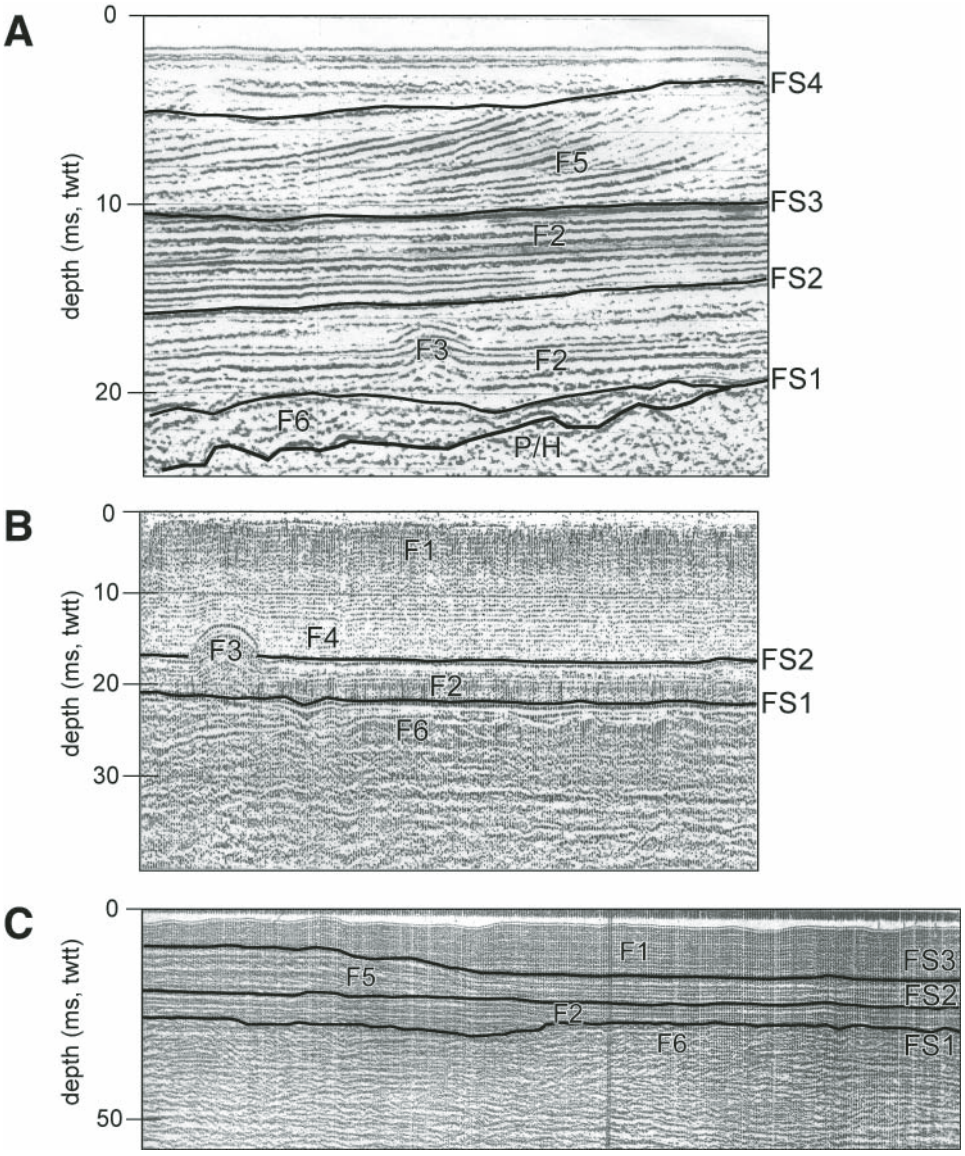

Figure 4. Illustration of the six major seismic facies and four major flooding surfaces recognized in this study: (A) selected facies for the U.S. Geological Survey boomer data, (B) selected facies for Rice University boomer data, and (C) selected facies for sparker data. twtt—two-way traveltime.

interpreted to represent fluvial-deltaic deposits that rest directly above the Pleistocene-Holocene contact. The U.S. Geological Survey Boomer data did not image this contact well when fluvial deposits rested above it. This is most likely due to the low impedance contrast between fluvial terrace deposits formed during the late Pleistocene fall in sea level and fluvial deposits formed during the Holocene rise in sea level. However, the lower-frequency boomer and sparker data did a better job imaging the Pleistocene-Holocene contact.

DISCUSSION

Bay Evolution

The general succession of facies within the deposits beneath Corpus Christi Bay illustrates an overall transgression. This general vertical succession of facies is punctuated by landward shifts in facies bounded by discrete flooding surfaces (sensu Anderson et al., 2001; transgressive overlap boundaries (TOBs) of Fletcher et al., 1993). Three, possibly four (FS1–FS4), major flooding surfaces occur. Flooding surfaces were observed in both seismic profiles and cores by sharp contacts between seismic and lithologic facies (Figs. 4 and 5). Radiocarbon ages from material above and below the flooding surfaces suggest that they formed in as little as 200 yr. Paleogeographic maps were constructed based on the facies found between flooding surfaces.

Pleistocene-Holocene Structure Map

The first task undertaken in this study was the identification and mapping of the Pleistocene-Holocene contact (sequence boundary) beneath the deposits of Corpus Christi Bay. This irregular surface is the antecedent topography that was flooded during

the transgression and represents the incised valley of the Nueces River that formed during the fall in sea level that culminated during the Last Glacial Maximum at 20 ka (Wright, 1980; Eckles et al., 2004; Simms et al., 2006b). In seismic profiles, this boundary was best delineated with sparker data. It was identified by reflectors that are erosionally truncated below and onlap above the surface (Mitchum et al., 1977; Fig. 6). In cores and seismic profiles, this surface represents the Pleistocene-Holocene boundary. This boundary was picked in Corp of Engineer boring descriptions as the contact between a soft or very soft gray mud or silty sand and a tan or gray stiff mud with calcareous nodules. Anything in the descriptions with pocket penetrometer values less than 1 (all values fell between 0.0 and 0.25) was assumed to be Holocene, while values measuring greater than 1 (all values were >2.0) were assumed to be Pleistocene. The contacts that were picked using this method matched remarkably well with the seismic interpretations and those from nearby rotary-drill cores. The map created using these methods is illustrated in Figure 7.

One prominent feature of the Pleistocene-Holocene surface is the steps observed in seismic profiles and cores (Fig. 6). The steps observed in the Pleistocene Holocene contact are interpreted to represent fluvial terraces that formed during the fall in sea level (120–20 ka). The same terraces have been mapped and dated using thermoluminescence dating in the lower portions of the Nueces River valley landward of the study area (Fig. 6B; Durbin et al., 1997).

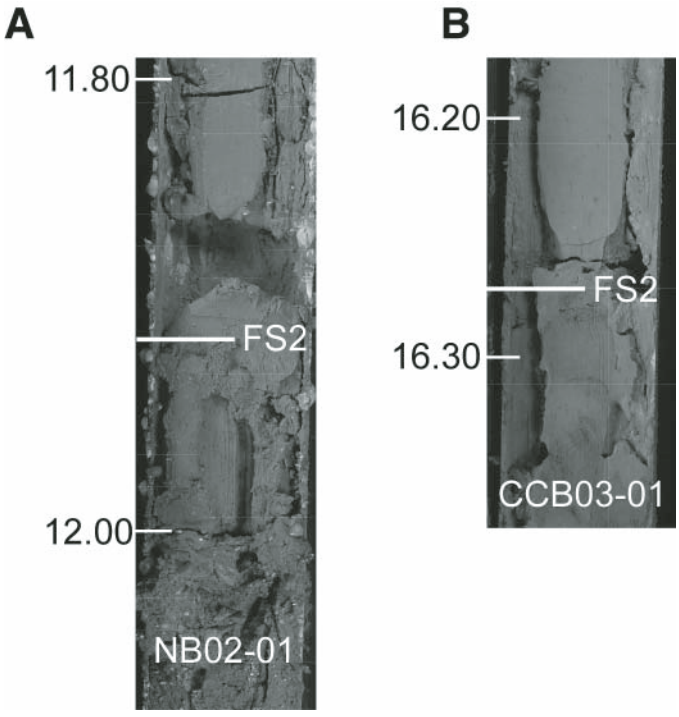

Figure 5. Core photographs of sharp lithological contacts between (A) facies SF2 and SF1 in core NB02-01 and (B) facies MF4 and MF1 in core CCB03-01, associated with the FS2 flooding surface. MF—mud facies; SF—sand facies.

Initial Drowning (FS1)

Seismic facies F6 lies directly above the Pleistocene surface and is interpreted as fluvial deposits of the Nueces River. A Texas Department of Transportation boring that sampled this unit was described by Wright (1980) as fining-upward coarse gravels to sand. These deposits lie above a large unconformity (our Pleistocene-Holocene structure map) interpreted by Wright (1980) to be the sequence boundary. The oldest bay deposits sampled in this study consist of lithofacies MF4 and correspond to seismic facies F2. These deposits lie above the fluvial coarse gravels and sands described by Wright (1980) and above a unit of SF2 interpreted to represent a mouth-bar environment. Two radiocarbon dates obtained from the bay unit resulted in ages of 9480 ± 1000 yr B.P. within CCB03-01 and 9650 ± 1040 yr B.P. within CCB02-01 (Figs. 8A and 8B). Seismic profiles indicate that the boundary between the underlying fluvial (F6) and upper bay (F2) deposits is sharp.

Flooding Surface 2 (FS2)

Based on radiocarbon dates in cores NB02-01, CCB02-01, and CCB03-01, FS2 formed around 8.0 ka (Fig. 8B). At this point, a large portion of central Corpus Christi Bay experienced a change from an upper-bay (seismic facies F2) to open-bay environment (F1 or F4), and, in places, these open-bay facies directly onlap Pleistocene strata (Fig. 6B). At the location of core CCB03-01, the lithofacies changes from MF4 to MF1 (Figs. 5 and 8A), marking a transition from an upper- to open-bay environment. Within cores NB02-01 and CCB02-01, the lithofacies changes from bayhead delta to upper bay (Figs. 5 and 8A). Figure 5 illustrates the sharp lithologic contacts that mark this flooding event. This change in lithology is also manifest in gamma-ray logs (Fig. 9). Prior to the formation of FS2, most oyster reefs (seismic facies F3) existed seaward of core CCB03-01. During this flooding event, they shifted landward to a location between core sites CCB03-01 and CCB02-01. These seismic and lithological changes represent back stepping of the upper-bay environment by 15 km in less than 200 yr (Figs. 10A and 10B).

Bayhead Delta Progradation

Around 6.8–7.0 ka, after FS2 but before FS3 formation, the bayhead delta of the Nueces River stopped retrograding and prograded into what is now Nueces Bay. In seismic profiles, clinoforms dipping both seaward and landward characterize this feature (Fig. 11). It has been interpreted as both a bayhead delta (Morton and Kindinger, 1998) and an interbay tidal-delta complex (Simms et al., 2003). Seismically, it has the attributes of a tidal-delta complex in that the clinoforms dip both landward and seaward. Several *Lucina amiantus* and *Crassinella lunulata* were sampled in other nearby shallow cores (i.e., hammer cores CCB94-8 and CCB94-9) from more seaward portions of the feature, suggesting proximity to an inlet or some other marine influence. Also, a fluvial feeder was not identified. However, long cores through the delta sampled plant fragments, along with restricted and more freshwater-influenced fauna (*Rangia*

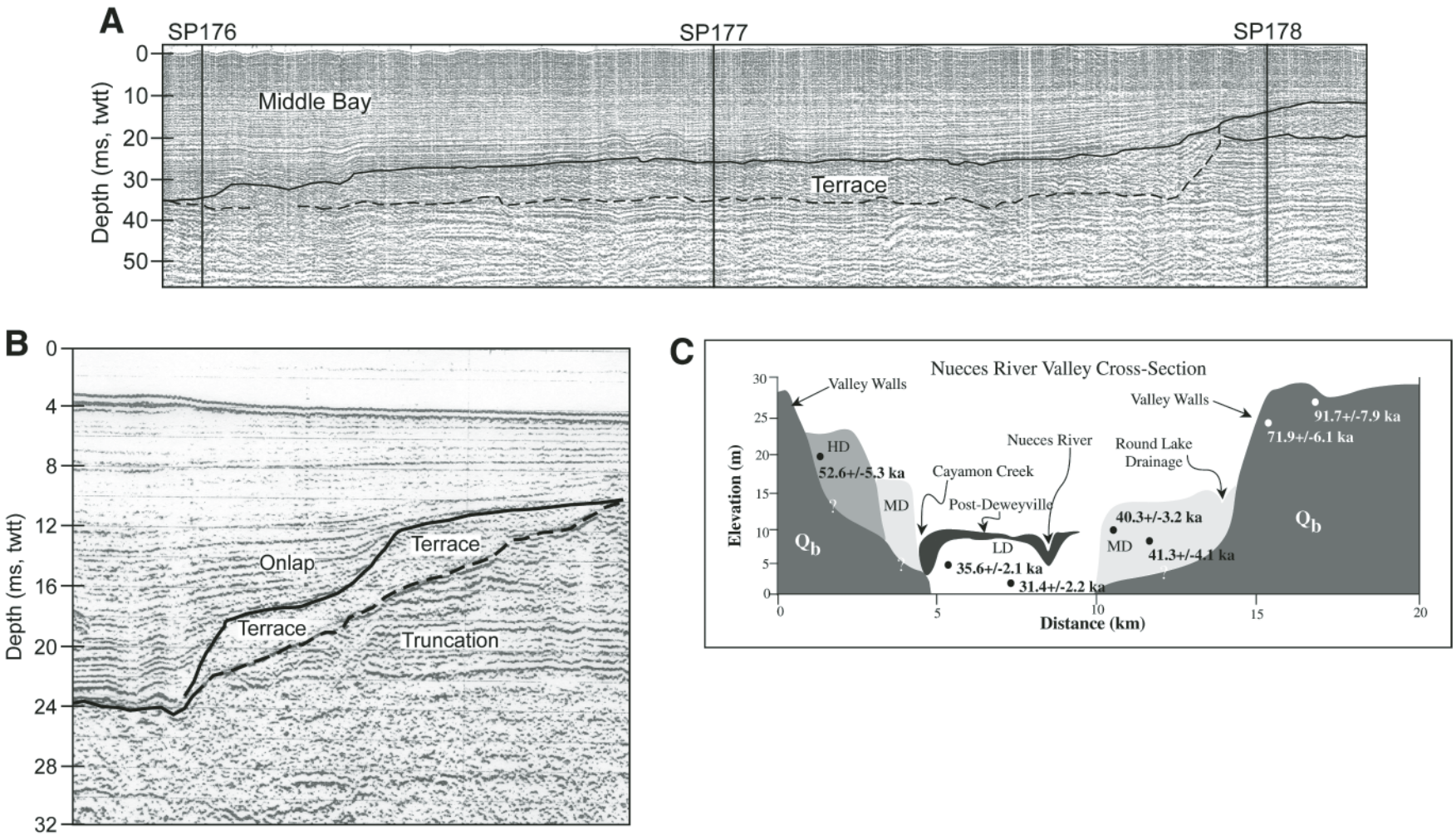

Figure 6. (A) Seismic line illustrating truncation below, onlap above, and distinct steps in the interpreted Pleistocene-Holocene contact. These steps are thought to be fluvial terraces formed during the last fall in sea level. (B) Fluvial terrace as illustrated in lower-resolution sparker profile. (C) Cross section of the Nueces River valley ~15 km updip from Corpus Christi Bay, illustrating fluvial terraces mapped on shore (Durbin et al., 1997). LD—Lower Deweyville; HD—High Deweyville; MD—Middle Deweyville; Qb—Quaternary Beaumont Formation; twtt—two-way traveltime.

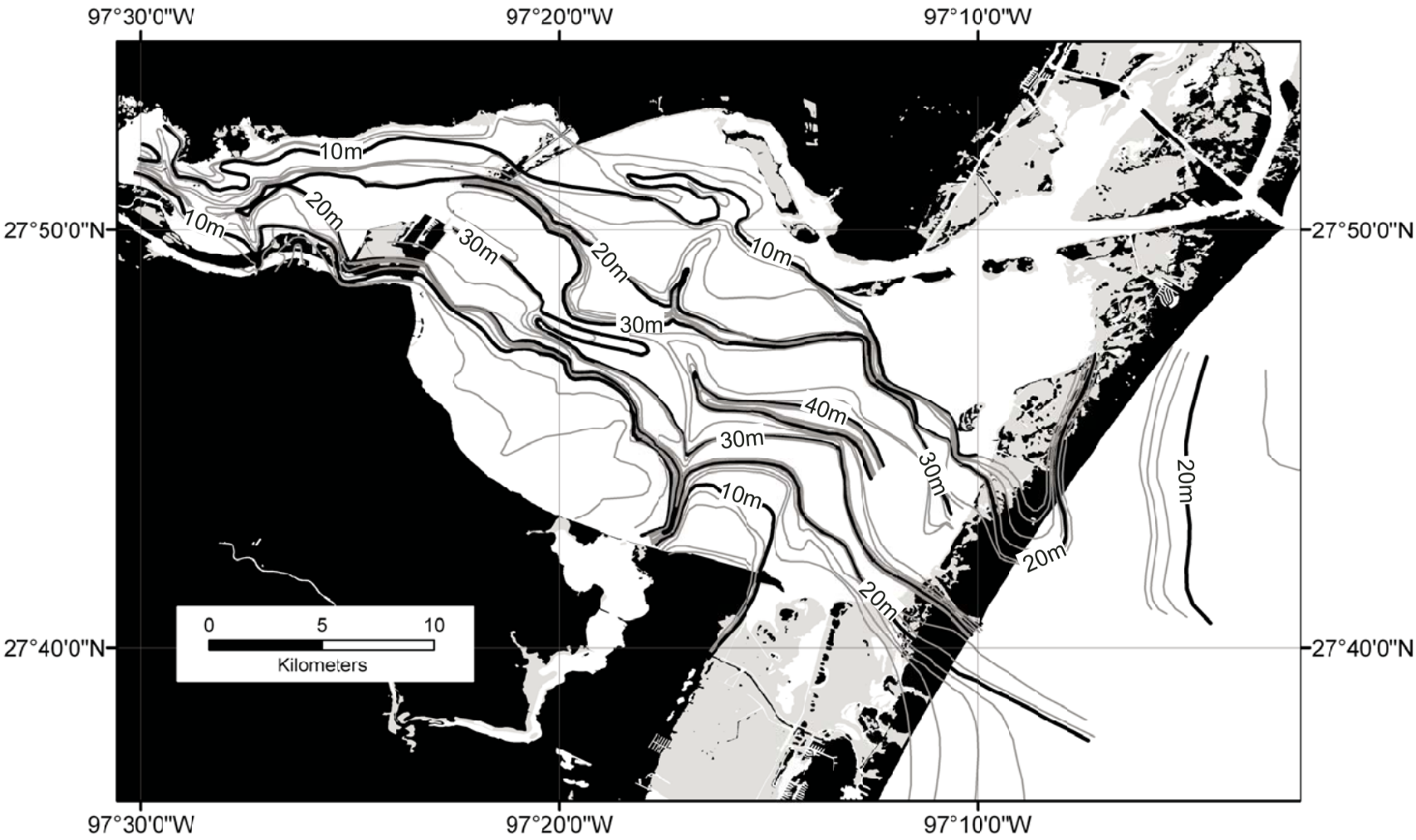

Figure 7. Elevation (meters below sea level) of the Pleistocene-Holocene contact beneath Corpus Christi Bay. Contour interval is 2 m.

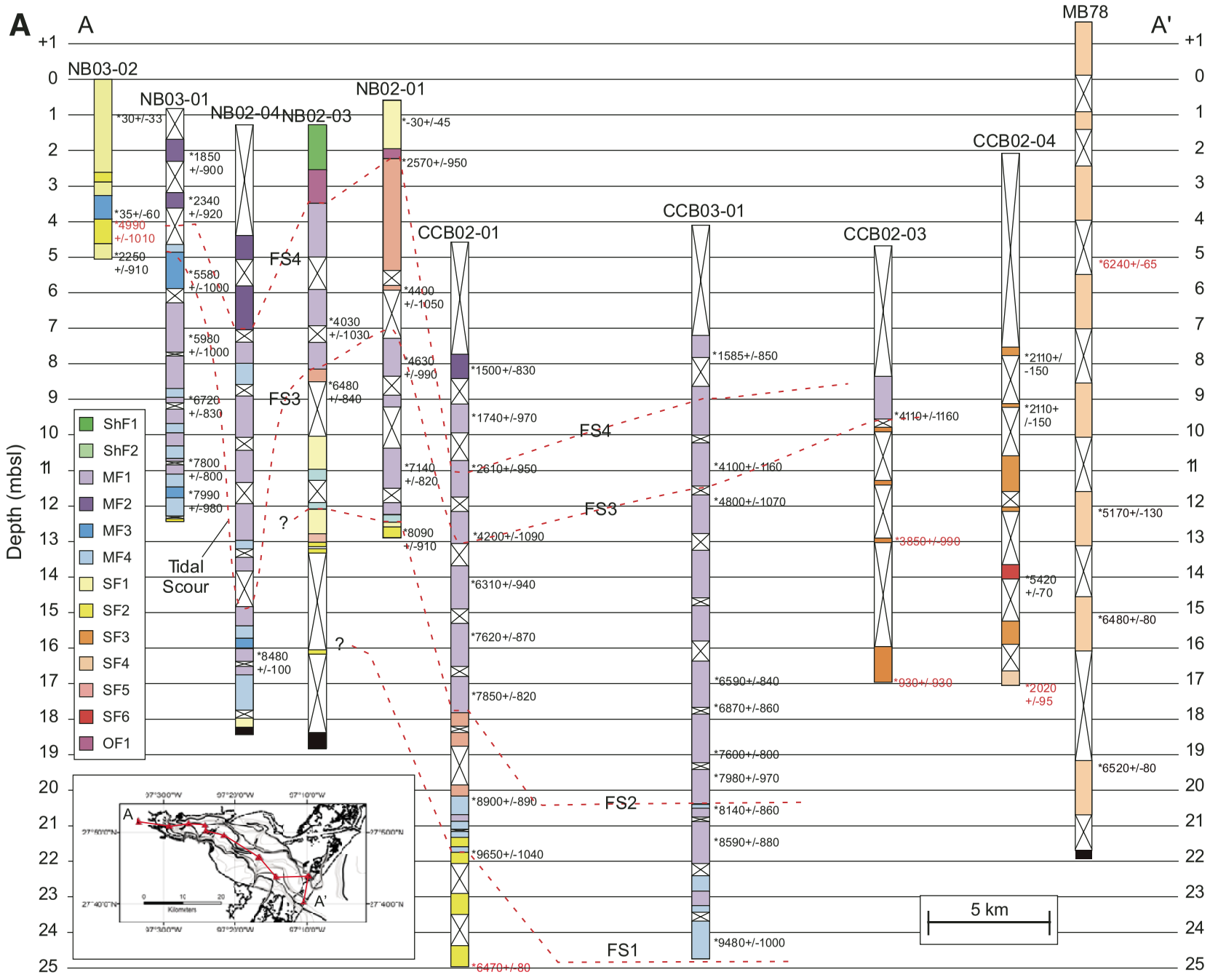

Figure 8 (*on this and following page*). (A) Dip-oriented core transect within Corpus Christi Bay illustrating lithofacies described in text. Dates in red are suspect.

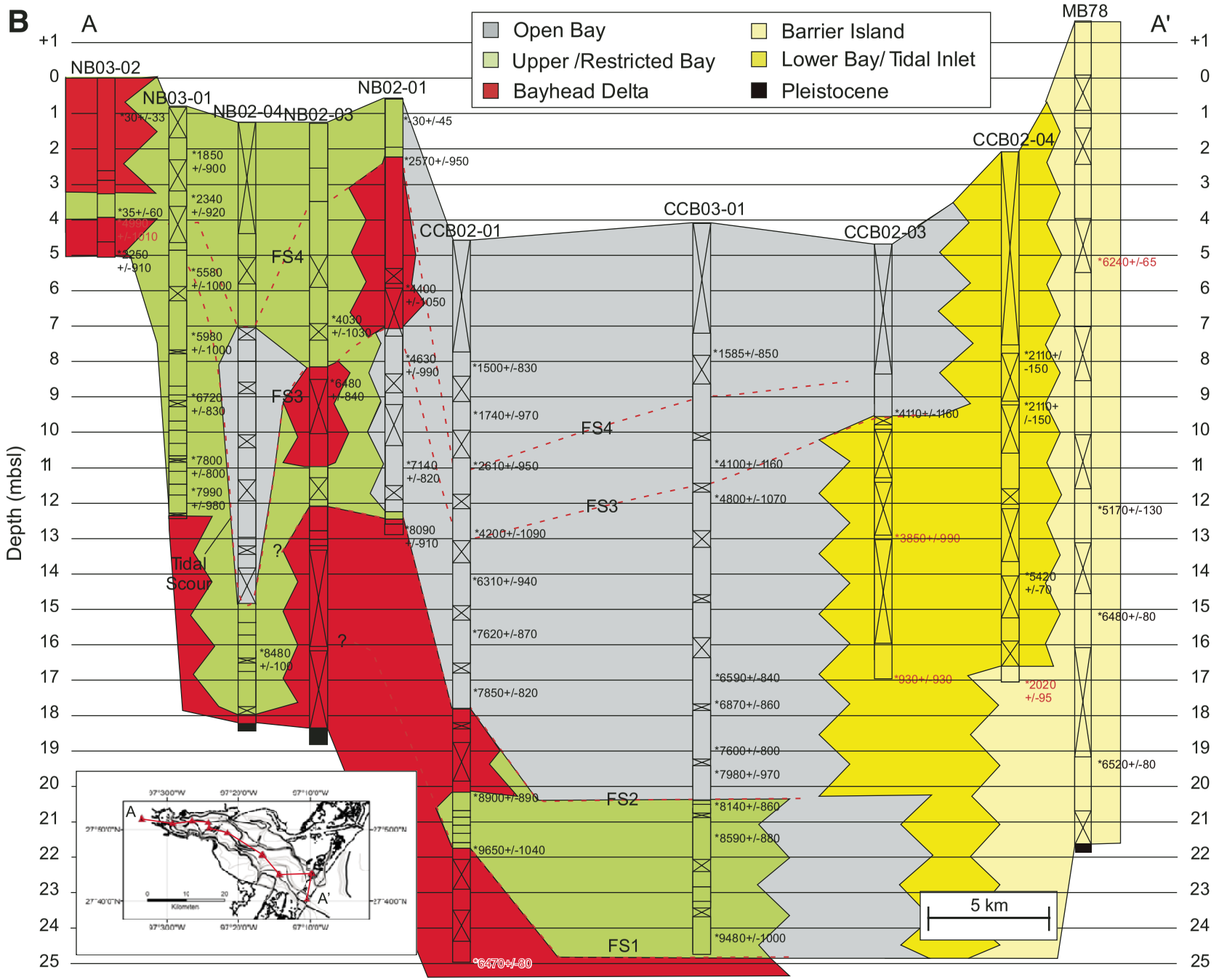

Figure 8 (*continued*). (B) Dip-oriented core transect within Corpus Christi Bay illustrating interpreted environments with isochrons. Dates in red are suspect. Dates in cal yr B.P. FS—flooding surface; MF—mud facies; SF—sand facies; ShF—shell-hash facies; OF—oyster reef facies.

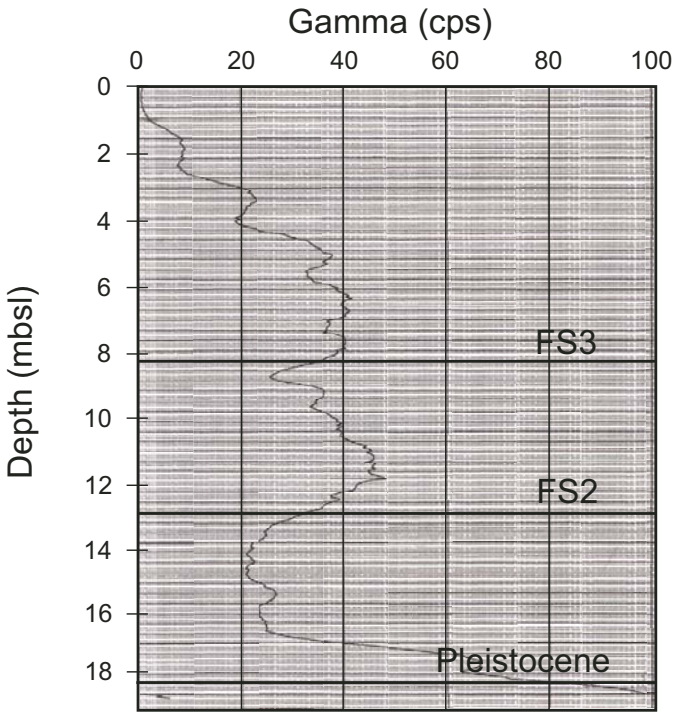

Figure 9. Gamma log from core NB02-03 illustrating the gamma response of flooding surfaces FS2 and FS3. Sands generally plot around 20 cps, and muds plot around 40–60 cps. Large values at base of hole indicate the Pleistocene.

flexuosa, *Macoma mitchelli*, etc.). In addition, core CCB94-10 sampled mouth-bar deposits (lithofacies SF2, Fig. 12A). Its coarse and lithic nature suggests proximity to a fluvial source. Core CCB94-12 contains *Lingulichnus* escape routes, which suggest rapid deposition (Fig. 12B). To account for these observations, we favor a tidally influenced bayhead delta interpretation. This interpretation would also explain the character of deposits within cores NB03-01, NB02-03, and NB02-04 at this time (Fig. 8A). A brackish lagoon would have existed landward of the bayhead delta in the vicinity of cores NB03-01, NB02-03, and NB02-04, explaining their more restricted fauna than open-bay environments but absence of sand and organic material found in a truly upper-bay and delta-influenced area. The fluvial feeder for the bayhead delta could be present beneath what is now the Port of Corpus Christi.

Tidal Delta

At some point after flooding surface FS2 formed, but prior to the formation of FS3, a tidal delta formed in the lower portions of the bay (Figs. 8B and 13). Cores sampling this feature contain SF6 and SF3 facies. This tidal delta is located 5 km from Mustang Island, which is believed to be in the same location now as it was then (Simms et al., 2006a). However, the absence of marine fauna within the delta does not suggest an open connection with the gulf, but rather connection with a shallow hypersaline bay. A possible explanation for the absence of marine fauna is a tidal delta associated with an inlet connecting a shallow lagoon landward of the open gulf with the open-bay environment of Corpus Christi Bay. This would also help to explain the tidal delta's large distance from Mustang Island.

Flooding Surface 3 (FS3)

Based on radiocarbon dates in cores NB02-03, NB02-01, CCB02-01, and CCB03-01, FS3 formed around 4.8 ka and in less than 700 yr (Fig. 8B). Within seismic profiles, this surface is marked by a shift in the location of the Nueces bayhead delta. Concurrent with that change in delta location, a large amount of erosion associated with FS3 occurred to the north of the new location of the bayhead delta (Fig. 14). In addition, a tidal-delta complex located in the lowermost portion of the bay terminates at FS3. Chronostratigraphically, the termination of the tidal delta is not as well constrained as the shift in location of the bayhead delta. Within core NB02-03, FS3 is manifest by a change from bayhead delta (SF5) to upper bay (MF1; Fig. 8A). Within core NB02-01, the contact at FS3 is not as abrupt as at FS2, but in the seismic profile through this core site, FS3 shows a prominent downlap surface associated with it (Fig. 15). The gradual lithologic change across FS3 in core NB02-01 is most likely due to the core's location in the distal portion of the bayhead delta (Figs. 8A and 15). In a more proximal location within the bayhead delta, this contact might be more abrupt. In the middle portions of the bay, such as at core locations CCB02-01 and CCB03-01, FS3 has no major lithologic changes associated with it and is often hard to map in seismic profiles. However, the location of oyster reefs shifted from the area between core sites CCB02-01 and CCB03-01 to behind present Rincon and Indian Points after the formation of FS3 (Fig. 1). At some point before FS3, but culminating after FS3, oyster reefs began to colonize the flanks of the bayhead delta (Fig. 16).

Flooding Surface 4 (FS4)

Based on radiocarbon dates in cores NB02-01, NB03-01, and CCB02-01, flooding surface FS4 formed around 2.6 ka (Fig. 8B). This event is marked by a large-scale back stepping of the Nueces bayhead delta. In core NB02-01 and NB02-03, oyster reefs replace delta-front and open-bay environments, respectively (Fig. 8A). Although the bayhead delta steps back to a location outside of the seismic coverage, lithofacies changes in core NB03-02 and reports by Brown et al. (1976) indicate that upper-bay or open-bay environments extended 10 km landward of the present bayhead delta ca. 2 ka. The locations and ages of these deposits suggest that the bayhead delta stepped back more than 20 km in less than a few centuries. Another change that occurred after FS4 is the appearance of lithological facies MF2 (Fig. 8A). MF2 is marked by discrete layers of shell material interpreted to represent storm beds. MF2 also contains a marked increase in sand without a decrease in sedimentation rates within the open-bay environments (Fig. 5). The large increase in percent sand in cores CCB02-01 and CCB03-01 is not as well constrained chronostratigraphically

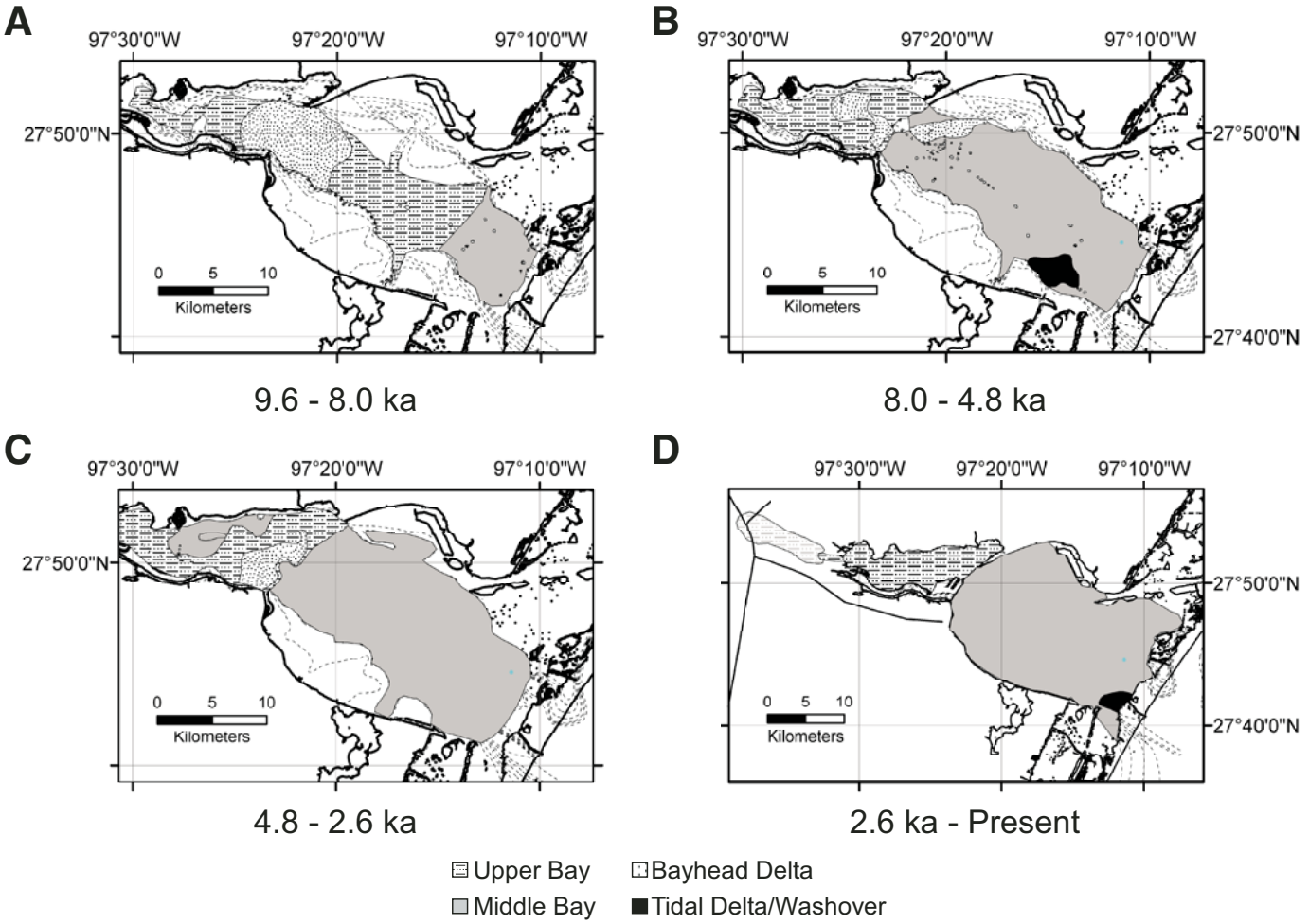

Figure 10. Paleogeography of Corpus Christi Bay illustrating environmental changes that occurred between each flooding surface. (A) Paleogeography prior to FS2 (8 ka), (B) paleogeography after FS2 but prior to FS3 (8–4.8 ka), (C) paleogeography after FS3 but prior to FS4 (4.8–2.6 ka), and (D) paleogeography after FS4 (2.6 ka).

as other changes at this time. The increase in percent sand is ubiquitous throughout the bay and does not show an increasing trend landward. This suggests a source for the sand other than the fluvial bayhead delta. This sand could possibly have been derived from wave erosion of sandy Pleistocene deposits lining the bayshore. This event does not mark any other distinct changes in the lower portions of the bay (i.e., CCB03-01).

Present Day

Over the last 2.6 ka and after FS4 formation, the bayhead delta of the Nueces River prograded to its present location (a distance of 10 km). The overstepped portions of the Nueces bayhead delta have been reworked into the present Rincon and Indian Points, effectively isolating Nueces Bay from Corpus Christi Bay, although this isolation has existed since the progradation of the delta around 7 ka. In addition, since the establishment of Indian and Rincon Points, an internal bay inlet has been established. This feature is characterized in cores by a coarse oyster shell hash (ShF1, Fig. 3). In seismic profiles, the area of the inlet is characterized by narrow cuspate ridges, possibly representing large-scale sediment waves (Fig. 11C). The processes that formed the inlet connecting Corpus Christi and Nueces Bay were more likely wind tides rather than true astronomical tides, since the tidal range within the bays is small (<0.3 m), and the winds along the central Texas coast and within Corpus Christi Bay have been shown to play the dominant role in sedimentation (Lohse, 1956; Shideler, 1984). Oyster reefs today occur only within Corpus Christi Bay, a product of the bay's salinity structure and distribution of suspended sediment (White et al., 1983).

Causes of Flooding Events

Several possible mechanisms could explain the multiple flooding events recorded in Corpus Christi Bay. These include tectonics, sea-level fluctuations, climate change, and autocyclic events, such as the flooding of antecedent topography and

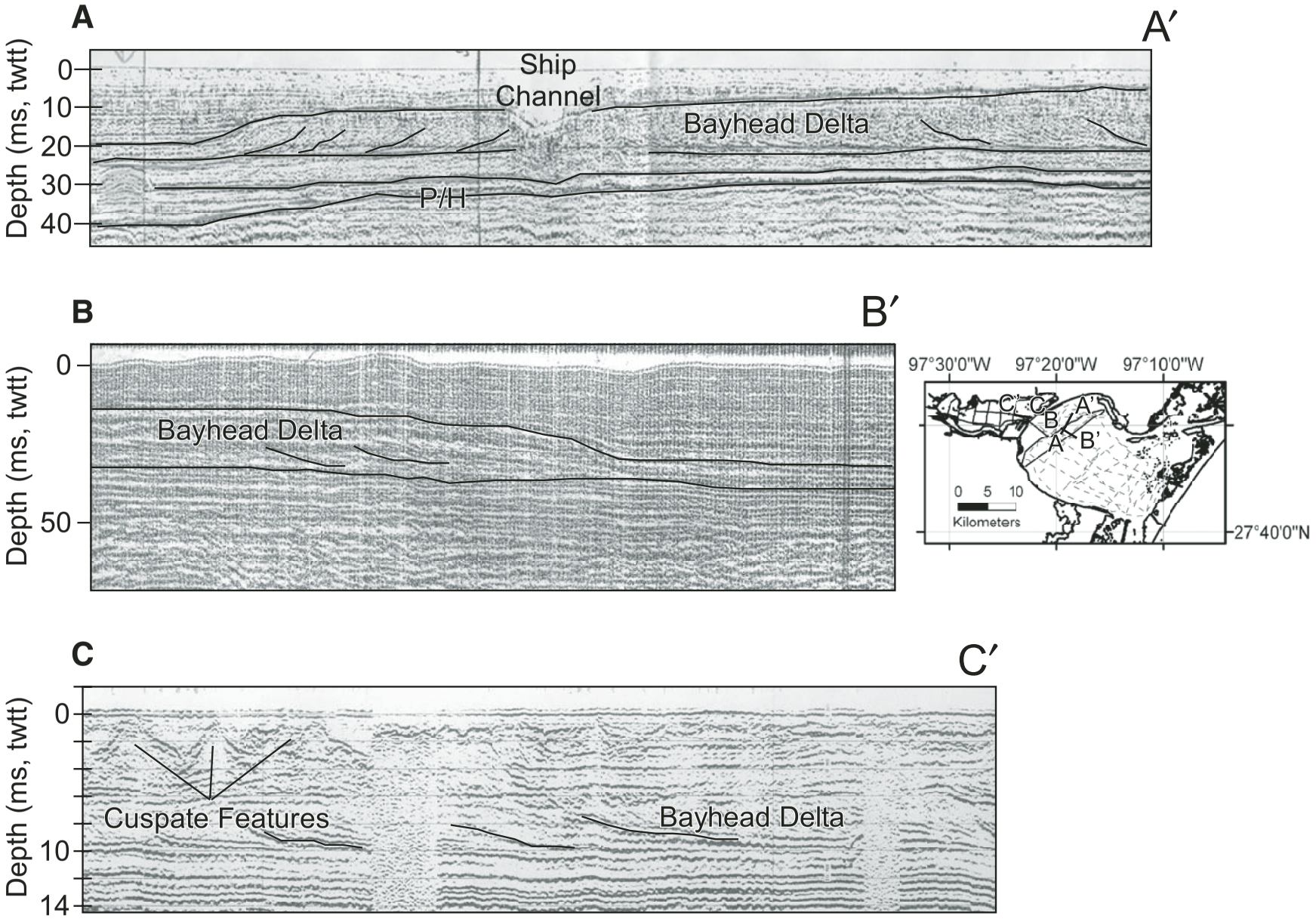

Figure 11. Seismic lines illustrating clinoforms associated with the progradation of the Nueces bayhead delta. In lines B–B′ and C–C′, the delta progrades both seaward and landward respectively, indicating a progradation direction for the bayhead delta orthogonal to the valley wall. Line C–C′ also illustrates the cuspate features associated with the inlet between Rincon and Indian Points separating Nueces and Corpus Christi Bay. P/H—Pleistocene-Holocene boundary; twtt—two-way traveltime.

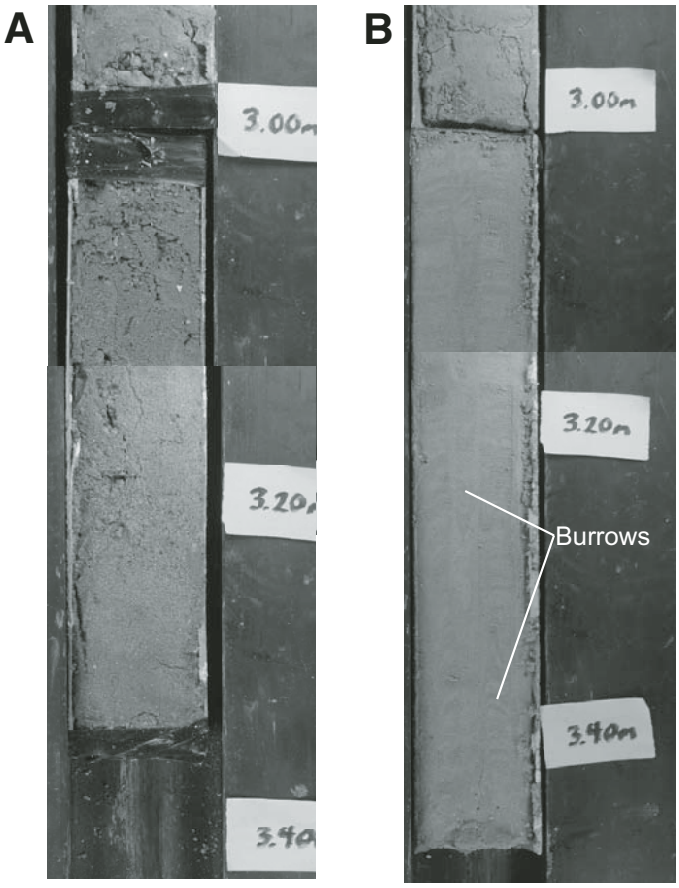

Figure 12. Photographs of (A) CCB94-10 illustrating sand facies 2 (SF2) and (B) burrowed unit in CCB94-12.

changes to the barrier-island system separating the estuary from the open gulf.

Tectonics

The only tectonic activity reported in this area is growth faulting (Price, 1933; Hillenbrand, 1985; Berryhill et al., 1986). Of these, only the Viola fault is thought to be active at the surface and not the result of hydrocarbon and groundwater withdrawal (Price, 1933; Hillenbrand, 1985). The Viola fault displaces one of the "Deweyville" terraces, named the Corpus Christi terrace (dated at 52.6 ± 5.3 ka by Durbin et al., 1997), in the upper reaches of Nueces Bay near Whites Point (Price, 1933). A seismic profile through the probable location of the Viola fault trace reveals no deformation of Holocene strata (Fig. 17). Although tectonic activity landward of the study area cannot be ruled out, it is thought that tectonic processes have not played an important role in the Holocene evolution of Corpus Christi Bay.

Changes to the Barrier-Island System

Mustang Island separates Corpus Christi Bay from the open Gulf of Mexico. It is thought to have aggraded in nearly the same location with little change for at least the last 7.5 k.y., possibly 9.5 k.y. (Shideler, 1986; Simms et al., 2006a). This is not to say changes such as the enlargement and migration of tidal inlets have not occurred. Within several of the short cores (CCB94-8, CCB94-13) from the northern margin of the bay, marine fauna (i.e., *Lucina* sp.) are more abundant than in modern deposits, suggesting a period of greater marine influence in the near past. However, Mustang Island at no point in its history disappeared altogether, and it has been near its present location during the entire time period of this study.

Flooding of Antecedent Topography

The Nueces River was in the same location during the marine isotope stage (MIS) 5e to 2 fall in sea level as it is today (Wright, 1980; Shideler, 1986; Durbin et al., 1997; Simms et al., 2006b). Terraces that formed during the fall in sea level, "Deweyville" terraces (Blum et al., 1995), are preserved along the Nueces River valley landward of Corpus Christi Bay (Durbin et al., 1997). Depositional remnants of these same terraces are preserved beneath the Holocene fill of Corpus Christi Bay (Figs. 6, 7, and 15). As sea level rose, the terraces were inundated. Each of the terraces has a gradient less than the average gradient of the base of the Nueces valley (Durbin et al., 1997). With each inundation of a terrace, the area of the estuary would increase at a higher rate, even at a constant rate of sea-level rise. For example, with the inundation of the −18 m terrace, the area of the bay increased by ~50% (260 km^2 compared to 170 km^2). These flooding events undoubtedly resulted in dramatic environmental changes caused by the reorganization of currents, salinity structures, etc. (Rodriguez et al., 2005). Given a constant rate of sediment flux spread over a larger area, slower aggradation rates would have occurred within upper-bay environments. This would help to explain the dramatic back stepping associated with FS2 (Figs. 10A and 10B). In addition, a large increase in the volume of water resulting from the flooding of a much larger bay area would increase the tidal prism coming into and out of the estuary. This could help explain the appearance of the large tidal delta after FS2. We suggest that the flooding of fluvial terraces played an important role in the flooding and formation of FS2 and FS3.

Sea-Level Changes

Sea-level rise was the first-order control on the evolution of Corpus Christi Bay. In general, the bay back stepped throughout the late Pleistocene and into the early and middle Holocene. The slowdown in the rate of sea-level rise around 5.5 ka was also coincident with the progradation of the Nueces bayhead delta. The events that caused the three major flooding surfaces, if controlled by sea level, would imply increasing rates of sea-level rise at 8.0 ka, 4.8 ka, and 2.6 ka. However, with the exception of the possible synchronous nature of FS2 with the 8.2 ka event associated with the draining of Lake Agassiz (Alley et al., 1997; Törnqvist et al., 2004b), during these time periods, the rate of sea-level rise was actually decreasing. For this reason, we interpret flooding surfaces FS3 and FS4 as resulting from other mechanisms,

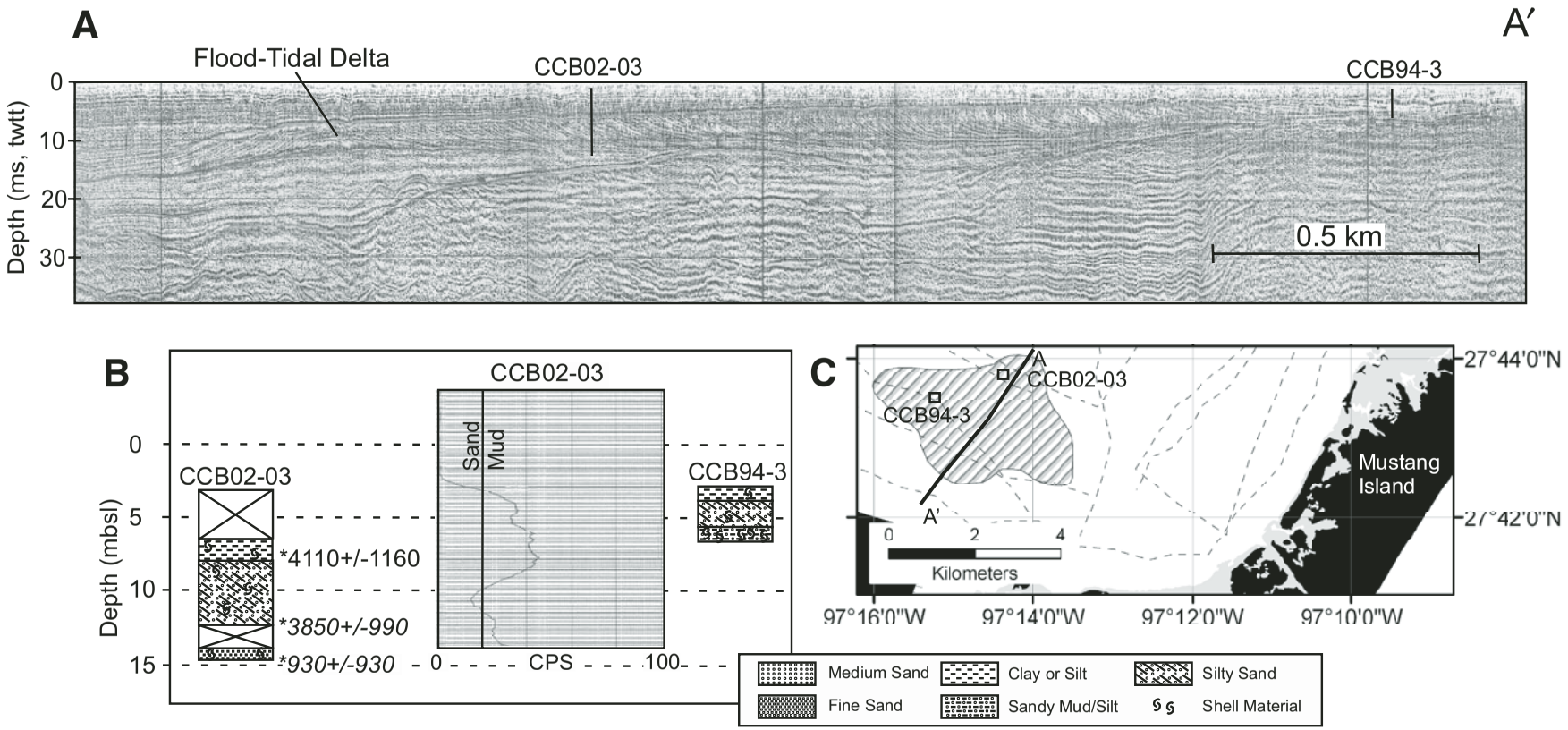

Figure 13. (A) Seismic line (A–A′) and lithology log and gamma log of cores (B) from an interpreted flood-tidal delta within Corpus Christi Bay. Seismic profile is oriented in a shore-parallel direction (C). In dip transects, the forests of the clinoforms dip landward. Core CCB02-03 sampled the more sandy flood-tidal delta and was used to constrain its age. Core CCB94-3 sampled the muddy distal edge of the delta. Within the gamma log, intervals measuring less than 20 cps are generally sandy, and those over 40 cps are muddy (from Simms et al., 2006a). Ages in cal yr B.P.

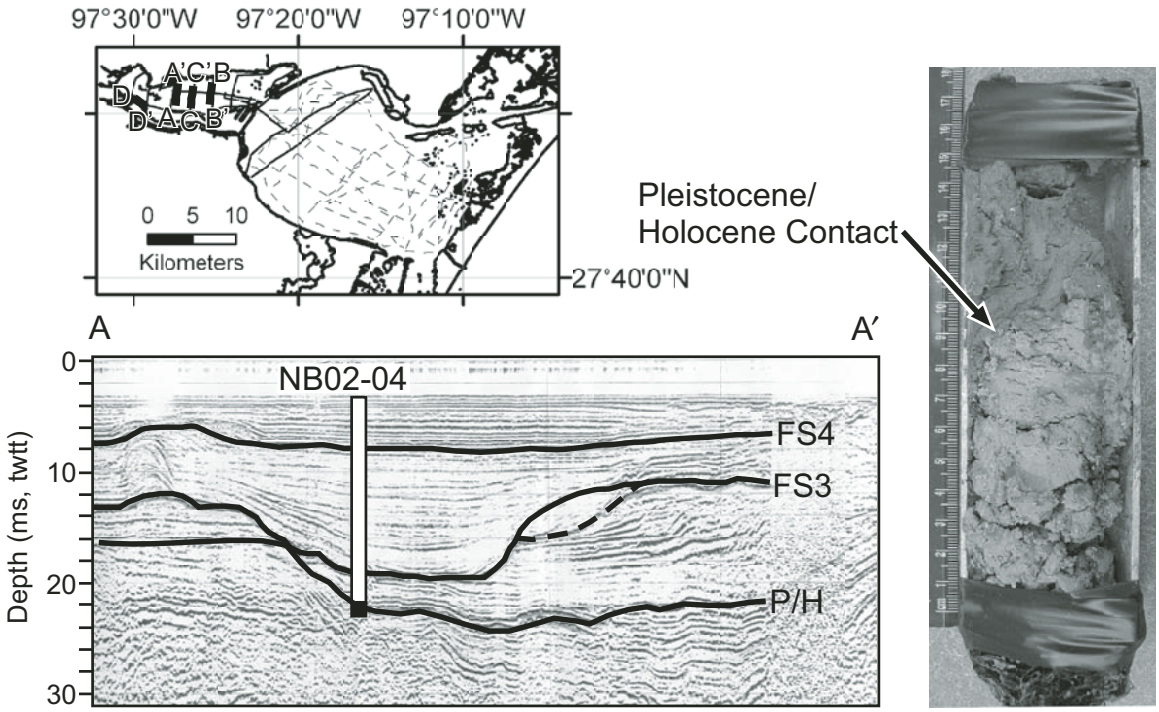

Figure 14. Seismic profile and core illustrating erosion along flooding surface FS3 that is interpreted to represent bay line ravinement possibly enhanced by a restriction between the newly avulsed delta lobe of the Nueces Delta and the edges of the Nueces paleovalley. P/H—Pleistocene-Holocene boundary; twtt—two-way traveltime.

such as climate change and the flooding of antecedent topography, rather than increases in the rate of sea-level rise. Still, it is not possible to rule out higher-order oscillations in sea level in the formation, as has been proposed by Mörner (1980), Fletcher et al. (1993), Suku and Pizzuto (1995), Donoghue and White (1995), and Froede (2002).

Climate Change

Much work has been done to reconstruct the late Quaternary climatic history of Texas (Bryant, 1977; Patton and Dibble, 1982; Bryant and Holloway, 1985; Toomey et al., 1993; Goodfriend and Ellis, 2000; Cooke et al., 2003). Unfortunately, little has been done along the Texas coast itself. The closest climate records to the study area are from cave deposits of the Edward's Plateau of central Texas (Toomey et al., 1993; Goodfriend and Ellis, 2000; Cooke et al., 2003; Ellwood and Gose, 2006). These records suggest that central Texas was cooler and effectively wetter at the end of the Pleistocene between 18 and 10.5 ka, and the early and middle Holocene experienced warmer and effectively drier conditions (Toomey et al., 1993). The effectively driest conditions occurred between 5 and 2.5 ka (Toomey et al., 1993). Recent work by Cooke et al. (2003) suggests that this event may have occurred a little earlier. Following the arid middle Holocene, the late Holocene brought higher effective moisture and somewhat cooler temperatures to the region, with a few possible higher-frequency climatic oscillations occurring around 1 ka.

An important outcome of the Toomey et al. (1993) work concerns the extent and timing of degradation of upland soils. They suggest that the soils of the Edward's Plateau began to be stripped around 8 ka and disappeared altogether by 2.5 ka. The nature and timing of these events would help to explain the progradation and ultimate back stepping of the Nueces bayhead delta. Coincident with a slowdown in the rate of sea-level rise, the stripping of soils from central Texas would provide the needed increase in sediment supply to prograde the bayhead delta. The disappearance of these soils by 2.5 ka is consistent with the dramatic back stepping of the bayhead delta around 2.6 ka. Changes in the grain size of Holocene terrace deposits along the Nueces River upstream from Corpus Christi Bay also reflect the stripping of upland soils (Durbin, 1999), although the role of fluvial storage and residence time within the Nueces River valley is unconstrained (Phillips and Slattery, 2006). In addition, the middle Holocene dry period would help to explain the presence of oysters within the Nueces bayhead delta and the appearance of *Anomalocardia cuneimeris* (a mollusk found in high-salinity bays further to the south of Corpus Christi Bay today) in lower-bay deposits during this time period.

Accompanying the climate changes around 2.5 ka, the winds across the central Texas coast could have changed to their present configuration. Models by Toomey et al. (1993) suggest that before this time, winds would have had a more southerly component and less of a southeasterly component. In conjunction with a slower rate of sea-level rise, a shift in winds around

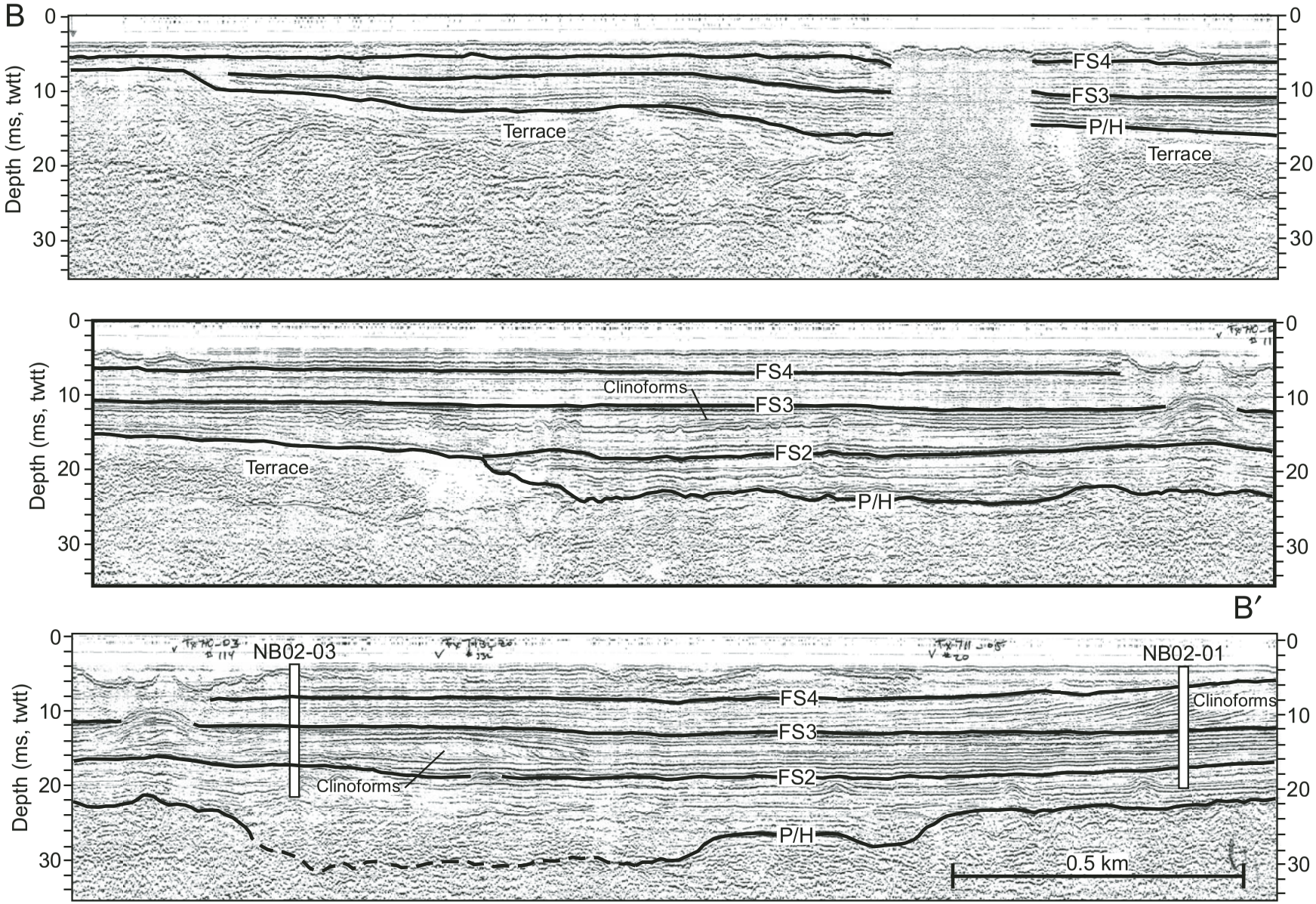

Figure 15. Seismic profile of U.S. Geological Survey 1996 line 14 illustrating the clinoforms of the bayhead delta and the location of cores NB02-01 and NB02-03 on the same seismic profile. See Figure 14 inset for line location. P/H—Pleistocene-Holocene boundary; FS—flooding surface; twtt—two-way traveltime.

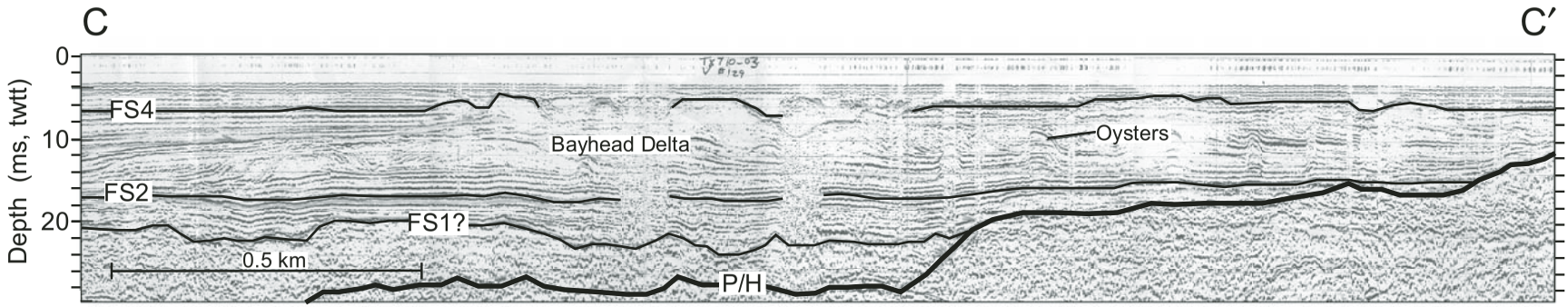

Figure 16. Seismic profile U.S. Geological Survey 1996 line 6 illustrating interpreted oyster reefs growing within the bayhead delta. See Figure 14 inset for line location. P/H—Pleistocene-Holocene boundary; FS—flooding surface; twtt—two-way traveltime.

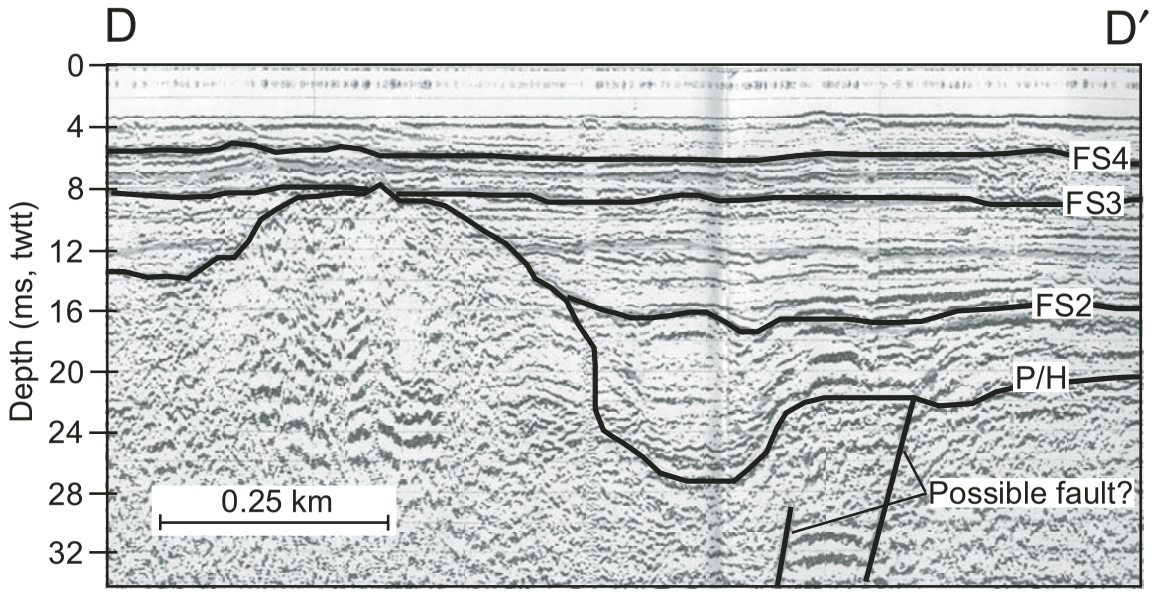

Figure 17. Seismic profile U.S. Geological Survey 1996 line 5, which passes through the fault trace of the Viola fault, is used to illustrate the lack of offset of Holocene strata. See Figure 14 inset for line location. P/H—Pleistocene-Holocene boundary; FS—flooding surface; twtt—two-way traveltime.

2.5 ka to a more southeasterly direction would allow for more erosion of sandy bay margins, explaining the ubiquitous increase in percent sand found in deposits throughout the bay since FS4 time. In addition, the climate change around 2.5 ka might have also brought about the current high hurricane frequency along the Gulf Coast, which would explain the appearance of the first discrete storm beds of lithofacies MF2.

CONCLUSIONS

Corpus Christi Bay occupies the flooded mouth of the ancestral Nueces River valley. The deposits within the bay provide an excellent record of the response of coastal environments to changes in sea level, climate, and local forcing mechanisms over the last 9.6 k.y., and they provide insights into how coastal systems may respond to future sea-level and climatic changes. These changes occurred during an overall sea-level rise but were punctuated by periods of rapid change. Three, possibly four, such rapid changes occurred at 9.6 ka, 8.0 ka, 4.8 ka, and 2.6 ka. At 8.0 ka, the upper-bay environment back stepped over 15 km, and oyster reefs were displaced 10 km to the north. At 4.8 ka, the bayhead delta of the Nueces River shifted to a new location, and a tidal inlet located in the southeast portion of the bay abruptly closed. In addition, oyster reefs started to colonize the Nueces bayhead delta. Around 2.6 ka, the Nueces bayhead delta back stepped over 20 km, well updip of its present location.

The 8.0 ka flooding event is interpreted to be the result of the flooding of fluvial terraces preserved beneath the Holocene fill of Corpus Christi Bay and possibly coinciding with the 8.2 ka eustatic event associated with the draining of Lake Agassiz. The 4.8 ka flooding event is interpreted to have resulted from a combination of a change in climate at the culmination of the middle Holocene dry period and the flooding of another fluvial terrace. The final event (2.6 ka) is thought to have been the result of a significant reduction in sediment supply following the stripping of upland soils and reestablishment of vegetation accompanying a climate change to more humid conditions.

ACKNOWLEDGMENTS

The authors would like to thank Jack Kindinger, Charles Holmes, and Nancy Soderberg at the U.S. Geological Survey for acquiring and allowing use of the two seismic surveys shot by the U.S. Geological Survey. We would also like to thank Mike Blum at Louisiana State University (LSU) for providing the nine long cores on Mustang Island. Patrick Taha, Chip Anderson, and Jessica Maddox helped in collecting cores within Corpus Christi Bay. Hermann Diaz from the Rice University geographic information systems (GIS) center helped with mapping and use of ArcView GIS. We would also like to thank the U.S. Army Corp of Engineers in Galveston, Texas, for allowing access to lithological descriptions of borings taken within Corpus Christi and Nueces Bays. James MacEachern helped to identify the trace fossils in core CCB94-12. James Durbin and Cecile Baeteman provided helpful reviews that greatly improved this manuscript. This work was funded by National Science Foundation (NSF) grant EAR-0107650, a National Science Foundation Graduate Fellowship, GCSSEPM Ed Picou Student Research Grant, ConocoPhillips, and ExxonMobil. This is Instituto di Geologia Marina (IGM) scientific contribution 1580.

REFERENCES CITED

Abdulah, K.C., 1995, The Evolution of the Brazos and Colorado Fluvial/Deltaic Systems during the Late Quaternary: An Integrated Study, Offshore Texas: Houston, Rice University, 284 p.

Alley, R.B., Mayewski, P.A., Sowers, T., Stuiver, M., Taylor, K.C., and Clark, P.U., 1997, Holocene climatic instability: A prominent, widespread event 8200 yr ago: Geology, v. 25, p. 483–486, doi: 10.1130/0091-7613(1997)025<0483:HCIAPW>2.3.CO;2.

Anderson, J.B., Rodriguez, A.B., Fletcher, C., and Fitzgerald, D., 2001, Researchers focus attention on coastal response to climate change: Eos (Transactions, American Geophysical Union), v. 82, p. 513, 519–520, doi: 10.1029/01EO00304.

Anderson, J.B., Rodriguez, A.B., Abdulah, K.C., Fillon, R.H., Banfield, L.A., McKeown, H.A., and Wellner, J.S., 2004, Late Quaternary stratigraphic evolution of the northern Gulf of Mexico margin: A synthesis, *in* Anderson, J.B., and Fillon, R.H., eds., Late Quaternary Stratigraphic Evolution of the Northern Gulf of Mexico Margin: Society for Sedimentary Geology (SEPM) Special Publication 79, p. 1–24.

Aten, L.E., 1983, Indians of the Upper Texas Coast: New York, Academic Press, 370 p.

Baeteman, C., Scott, D.B., and Van Strydonck, M., 2002, Changes in coastal zone processes at a high sea-level stand: A late Holocene example from Belgium: Journal of Quaternary Science, v. 17, p. 547–559, doi: 10.1002/jqs.707.

Bard, E., Hamelin, B., Arnold, M., Montaggioni, L., Cabioch, G., Faure, G., and Rougerie, F., 1996, Deglacial sea level record from Tahiti corals and the timing of global meltwater discharge: Nature, v. 382, p. 241–244, doi: 10.1038/382241a0.

Bartek, L.R., Cabote, B.S., Young, T., and Schroeder, W., 2004, Sequence stratigraphy of a continental margin subjected to low-energy and low-sediment-supply environmental boundary conditions: Late Pleistocene–Holocene deposition offshore Alabama, USA, *in* Anderson, J.B., and Fillon, R.H., eds., Late Quaternary Stratigraphic Evolution of the Northern Gulf of Mexico Margin: Society for Sedimentary Geology (SEPM) Special Publication 79, p. 85–109.

Belknap, D.F., and Kraft, J.C., 1981, Preservation potential of transgressive coastal lithosomes on the U.S. Atlantic shelf: Marine Geology, v. 42, p. 429–442, doi: 10.1016/0025-3227(81)90173-0.

Belknap, D.F., and Kraft, J.C., 1985, Influence of antecedent geology on stratigraphic preservation potential and evolution of Delaware's barrier systems: Marine Geology, v. 63, p. 235–262, doi: 10.1016/0025-3227(85)90085-4.

Berryhill, H.L., Suter, J.R., and Hardin, N.S., 1986, Quaternary Facies and Structure, Northern Gulf of Mexico: Interpretations from Seismic Data: American Association of Petroleum Geology Studies in Geology, v. 23, 289 p.

Blum, M.D., Morton, R.A., and Durbin, J.M., 1995, "Deweyville" terraces and deposits of the Texas Gulf Coastal Plain: Transactions of the Gulf Coast Association of Geological Societies, v. 45, p. 53–60.

Blum, M.D., Misner, T.J., Collins, E.C., Scott, D.B., Morton, R.A., and Aslam, A., 2001, Middle Holocene sea-level rise and highstand at +2 m, central Texas coast: Journal of Sedimentary Research, v. 71, no. 4, p. 581–588, doi: 10.1306/112100710581.

Blum, M.D., Carter, A.E., Zayac, T., and Goble, R., 2002, Middle Holocene sea level and evolution of the Gulf of Mexico: Journal of Coastal Research, v. 36, Special Issue, p. 65–80.

Bratton, J.F., Coleman, S.M., Thieler, E.R., and Seal, R.R., II, 2003, Birth of the modern Chesapeake Bay estuary between 7.4 and 8.2 ka and implications for global sea-level rise: Geo-Marine Letters, v. 22, p. 188–197.

Brown, L.F., Brewton, J.L., McGowen, J.H., Evans, T.J., Fisher, W.L., and Groat, C.G., 1976, Environmental Geologic Atlas of the Texas Coastal

Zone—Corpus Christi Area: Austin, Bureau of Economic Geology, University of Texas at Austin, 123 p.

Bryant, V.M., 1977, A 16,000 year pollen record of vegetation change in central Texas: Palynology, v. 1, p. 143–156.

Bryant, V.M., and Holloway, R.W., 1985, The late Quaternary paleoenvironmental record of Texas, *in* Bryant, V.M. and Holloway, R.W., eds., Pollen Records of Late-Quaternary North American Sediments: Dallas, Texas, American Association of Stratigraphic Palynologists, p. 39–70.

Carr, J.T., 1967, The Climate and Physiography of Texas: Austin, Texas, Texas Water Development Board Report 53, 27 p.

Chappell, J., and Polach, H., 1991, Post-glacial sea-level rise from a coral record at Huon Peninsula, Papua New Guinea: Nature, v. 349, p. 147–149, doi: 10.1038/349147a0.

Coleman, J.M., and Smith, W.G., 1964, Late recent rise of sea level: Geological Society of America Bulletin, v. 75, p. 833–840, doi: 10.1130/0016-7606(1964)75[833:LRROSL]2.0.CO;2.

Cooke, M.J., Stern, L.A., Banner, J.L., Mack, L.E., Stafford, T.W., Jr., and Toomey, R.S., III, 2003, Precise timing and rate of massive late Quaternary soil denudation: Geology, v. 31, no. 10, p. 853–856, doi: 10.1130/G19749.1.

Curray, J.R., 1960, Sediments and history of Holocene transgression, continental shelf, northwestern Gulf of Mexico, *in* Shepard, F.P., Phleger, F.B., and van Andel, T.H., eds., Recent Sediments, Northwestern Gulf of Mexico: Tulsa, Oklahoma, American Association of Petroleum Geologists, p. 221–266.

Donoghue, J.F., and White, N.M., 1995, Late Holocene sea-level change and delta migration, Apalachicola River region, NW Florida, USA: Journal of Coastal Research, v. 11, p. 651–663.

Durbin, J.M., 1999, Geomorphic Response to Late Quaternary Climate and Sea Level Change, Lower Nueces River, Texas [Ph.D. thesis]: Lincoln, Nebraska, University of Nebraska, 242 p.

Durbin, J.M., Blum, M., and Price, D.M., 1997, Late Pleistocene stratigraphy of the lower Nueces River, Corpus Christi, Texas: Glacio-eustatic influences on valley-fill architecture: Transactions of the Gulf Coast Association of Geological Societies, v. 47, p. 119–129.

Ellwood, B.B., and Gose, W.A., 2006, Heinrich, HI and 8200 yr B.P. climate events recorded in Hull's Cave, Texas: Geology, v. 34, p. 753–756, doi: 10.1130/G22549.1.

Eckles, B.J., Fassell, M.L., and Anderson, J.B., 2004, Late Quaternary evolution of the wave-storm-dominated central Texas shelf, *in* Anderson, J.B., and Fillon, R.H., eds., Late Quaternary Stratigraphic Evolution of the Northern Gulf of Mexico Margin: Society for Sedimentary Geology (SEPM) Special Publication 79, p. 271–287.

Fairbanks, R.G., 1989, A 17,000-year glacio-eustatic sea level record: Influence of glacial melting on the Younger Dryas event and deep-ocean circulation: Nature, v. 342, no. 6250, p. 637–642, doi: 10.1038/342637a0.

Fletcher, C.H., Van Pelt, J.E., Brush, G.S., and Sherman, J., 1993, Tidal wetland record of Holocene sea-level movements and climate history: Palaeogeography, Palaeoclimatology, Palaeoecology, v. 102, p. 177–213, doi: 10.1016/0031-0182(93)90067-S.

Froede, C.R., Jr., 2002, Rhizolith evidence in support of a late Holocene sea-level highstand at least 0.5 m higher than at present Key Biscayne, Florida: Geology, v. 30, p. 203–206, doi: 10.1130/0091-7613(2002)030<0203:REISOA>2.0.CO;2.

Goodfriend, G.A., and Ellis, G.L., 2000, Stable carbon isotope record of Middle to Late Holocene climate changes from land snail shells at Hinds Cave, Texas: Quaternary International, v. 67, p. 47–60, doi: 10.1016/S1040-6182(00)00008-2.

Henley, D.E., and Rauschuber, D.G., 1981, Freshwater Needs of Fish and Wildlife Resources in the Nueces–Corpus Christi Bay Area, Texas: A Literature Synthesis: Washington, D.C., U.S. Fish and Wildlife Service, Office of Biological Services Report FWS/OBS-80/10, 410 p.

Hillenbrand, C.J., III, 1985, Subsidence and Fault Activation Related to Fluid Extraction Saxet Field, Nueces County, Texas: Houston, University of Houston, 144 p.

Lambeck, K., and Chappell, J., 2001, Sea level change through the last glacial cycle: Science, v. 292, p. 679–686, doi: 10.1126/science.1059549.

Lighty, R.G., Mcintyre, I.G., and Stuckenrath, R., 1982, *Acropora palmata* reef framework; a reliable indicator of sea level in the Western Atlantic for the past 10,000 years: Coral Reefs, v. 1, p. 125–130, doi: 10.1007/BF00301694.

Lohse, E.A., 1956, Dynamic geology of the modern coastal region, northwestern Gulf of Mexico, *in* Hough, J.L., ed., Finding Ancient Shorelines: A Symposium with Discussions: Society of Economic Mineralogists and Paleontologists (SEPM) Special Publication 3, p. 99–104.

Mannino, A., and Montagna, P.A., 1996, Fine-scale spatial variation of sediment composition and salinity in Nueces Bay of south Texas: The Texas Journal of Science, v. 48, no. 1, p. 35–47.

Marmer, H.A., 1954, Tides and sea level in the Gulf of Mexico, *in* Gulf of Mexico, Its Origin, Waters, and Marine Life: U.S. Department of Interior Fish Wildlife Service Bulletin, v. 89, p. 101–118.

McFarlan, E., Jr., 1961, Radiocarbon dating of late Quaternary deposits, South Louisiana: Geological Society of America Bulletin, v. 72, p. 129–158, doi: 10.1130/0016-7606(1961)72[129:RDOLQD]2.0.CO;2.

Mitchum, R.M., Jr., Vail, P.R., and Sangree, J.B., 1977, Seismic stratigraphy and global changes of sea level: Part 6. Stratigraphic interpretation of seismic reflection patterns in depositional sequences, *in* Payton, C.E., ed., Seismic Stratigraphy, Applications to Hydrocarbon Exploration: American Association of Petroleum Geology Memoir 26, p. 117–133.

Moore, D.G., and Scruton, P.C., 1957, Minor internal structures of some recent unconsolidated sediments: American Association of Petroleum Geologists Bulletin, v. 41, p. 2723–2751.

Mörner, N.A., 1980, The northwestern European "sea-level laboratory" and regional Holocene eustasy: Palaeogeography, Palaeoclimatology, and Palaeoecology, v. 29, p. 281–300, doi: 10.1016/0031-0182(79)90086-5.

Morton, R.A., and Kindinger, J.L., 1998, Responses of coastal systems to late Pleistocene and Holocene sea-level fluctuations, Corpus Christi Region: Corpus Christi, Texas, Gulf Coast Association of Geological Societies, Field Trip Guidebook, 24 p.

Morton, R.A., and McGowen, J.H., 1980, Modern Depositional Environments of the Texas Coast: Austin, Bureau of Economic Geology, The University of Texas at Austin, Guidebook 20, 167 p.

Morton, R.A., Paine, J.G., and Blum, M.D., 2000, Responses of stable bay-margin and barrier-island systems to Holocene sea-level highstands, western Gulf of Mexico: Journal of Sedimentary Research, v. 70, no. 3, p. 478–490, doi: 10.1306/2DC40921-0E47-11D7-8643000102C1865D.

Nelson, H.F., and Bray, E.E., 1970, Stratigraphy and history of the Holocene sediments in the Sabine-High Island area, Gulf of Mexico, *in* Morgan, J.P., eds., Deltaic Sedimentation Modern and Ancient: Society of Economic Paleontologists and Mineralogists (SEPM) Special Publication 15, p. 48–77.

Paine, J.G., 1993, Subsidence of the Texas Coast: Inferences from historical and late Pleistocene sea levels: Tectonophysics, v. 222, p. 445–458.

Patton, P.C., and Dibble, D.S., 1982, Archeologic and geomorphic evidence for the paleohydrologic record of the Pecos River in West Texas: American Journal of Science, v. 282, p. 97–121.

Peltier, W.R., Farrell, W.E., and Clark, J.A., 1978, Glacial isostasy and relative sea-level: A global finite element model: Tectonophysics, v. 50, p. 81–110, doi: 10.1016/0040-1951(78)90129-4.

Penland, S., Boyd, R., and Suter, J.R., 1988, Transgressive depositional systems of the Mississippi Delta Plain: A model for barrier shoreline and shelf sand movement: Journal of Sedimentary Petrology, v. 58, p. 932–949.

Phillips, J.D., and Slattery, M.C., 2006, Sediment storage, sea level, and sediment delivery to the ocean by coastal plain rivers: Progress in Physical Geography, v. 30, p. 513–530, doi: 10.1191/0309133306pp494ra.

Price, W.A., 1933, Role of diastrophism in topography of Corpus Christi Area: South Texas: American Association of Petroleum Geology Bulletin, v. 17, no. 8, p. 907–962.

Raymond, P.A., and Bauer, J.E., 2001, Riverine export of aged terrestrial organic matter to the North Atlantic Ocean: Nature, v. 409, p. 497–499, doi: 10.1038/35054034.

Rehkemper, J.L., 1969, Sedimentology of Holocene Estuarine Deposits, Galveston Bay, Texas: Houston, Rice University, 61 p.

Rodriguez, A.B., Anderson, J.B., Siringan, F.P., and Taviani, M., 2004, Holocene evolution of the east Texas coast and inner shelf: Along-strike variability in coastal retreat rates: Journal of Sedimentary Research, v. 74, p. 405–422, doi: 10.1306/092403740405.

Rodriguez, A.B., Anderson, J.B., and Simms, A.R., 2005, Terrace inundation as an autocyclic mechanism for parasequences formation, Galveston estuary, Texas: Journal of Sedimentary Research, v. 75, p. 608–618, doi: 10.2110/jsr.2005.050.

Shepard, F., 1953, Sedimentation rates in Texas estuaries and lagoons: American Association of Petroleum Geologists Bulletin, v. 37, p. 1919–1934.

Shepard, F., and Moore, D.G., 1954, Sedimentary environments differentiated by coarse-fraction studies: American Association of Petroleum Geology Bulletin, v. 38, no. 8, p. 1792–1802.

Shepard, F., and Moore, D.G., 1955, Central Texas coast sedimentation: Characteristics of sedimentary environment, recent history, and diagenesis: American Association of Petroleum Geology Bulletin, v. 39, no. 8, p. 1463–1593.

Shepard, F.P., and Suess, H.E., 1956, Rate of postglacial rise of sea level: Science, v. 123, p. 1082–1083, doi: 10.1126/science.123.3207.1082-a.

Shideler, G.L., 1984, Suspended sediment responses in a wind-dominated estuary of the Texas Gulf Coast: Journal of Sedimentary Petrology, v. 54, no. 3, p. 731–745.

Shideler, G.L., 1986, Seismic and physical stratigraphy of late Quaternary deposits, south Texas coastal complex, *in* Shideler, G.L., ed., Stratigraphic Studies of a Late Quaternary Barrier-Type Coastal Complex, Mustang Island–Corpus Christi Area, South Texas Gulf Coast: U.S. Geological Survey Professional Paper 1328-B, p. 9–31.

Simms, A.R., Anderson, J.B., and Rodriguez, A.B., 2003, The role of antecedent topography in shaping coastal change caused by sea-level rise: XVI International Union for Quaternary Research (INQUA) Congress, Programs and Abstracts, p. 239.

Simms, A.R., Anderson, J.B., and Blum, M.D., 2006a, Barrier-island aggradation via inlet migration, Mustang Island Texas: Sedimentary Geology, v. 187, p. 105–125, doi: 10.1016/j.sedgeo.2005.12.023.

Simms, A.R., Anderson, J.B., Taha, Z.P., and Rodriguez, A.B., 2006b, Overfilled versus underfilled incised valleys: Lessons from the Gulf of Mexico, *in* Dalrymple, R., Leckie, S., and Tillman, R., eds., Incised Valleys through Space and Time: Society for Sedimentary Geology (SEPM) Special Publication 85, p. 117–139.

Simms, A.R., Lambeck, K., Purcell, A., Anderson, J.B., and Rodriguez, A.B., 2007, Sea-level history of the Gulf of Mexico since the Last Glacial Maximum with implications for the melting history of the Laurentide Ice Sheet: Quaternary Science Reviews, v. 26, p. 920–940.

Simpson, R.H., and Lawrence, M.B., 1971, Atlantic hurricane frequencies along the US coastline: U.S. Department of Commerce, National Oceanic and Atmospheric Administration Technical Memorandum NWS SR-58.

Snedden, J.W., Nummedal, D., and Amos, A.F., 1988, Storm- and fair-weather combined flow on the central Texas shelf: Journal of Sedimentary Petrology, v. 58, no. 4, p. 580–595.

Sperazza, M., Moore, J.N., and Hendrix, M.S., 2004, High-resolution particle size analysis of naturally occurring very fine–grained sediment through laser diffractometry: Journal of Sedimentary Research, v. 74, p. 736–743, doi: 10.1306/031104740736.

Stapor, F.W., Jr., and Stone, F.W., 2004, A new depositional model for the buried 4000 yr BP New Orleans barrier: Implications for sea-level fluctuations and onshore transport from a nearshore shelf source: Marine Geology, v. 204, p. 215–234, doi: 10.1016/S0025-3227(03)00350-5.

Streif, H., 2004, Sedimentary record of Pleistocene and Holocene marine inundations along the North Sea coast of Lower Saxony, Germany: Quaternary International, v. 112, p. 3–28, doi: 10.1016/S1040-6182(03)00062-4.

Stuiver, M., and Braziunas, T.F., 1993, Modeling atmospheric ^{14}C influences and ^{14}C ages of marine samples to 10,000 B.C.: Radiocarbon, v. 35, no. 1, p. 137–189.

Stuiver, M., Reimer, P.J., Bard, E., Beck, J.W., Burr, G.S., Hughen, K.A., Kromer, B., McCormac, G., van der Plicht, J., and Spurk, M., 1998, INTCAL98 radiocarbon age calibration, 24,000–0 cal B.P.: Radiocarbon, v. 40, no. 3, p. 1041–1083.

Suku, J.J., and Pizzuto, J.E., 1995, Accelerated sea-level rise 2,000 years BP in the Delaware Bay and stratigraphic evidence from the Leipsic River valley, Delaware, USA: Journal of Coastal Research, v. 11, p. 573–582.

Sydow, J., and Roberts, H.H., 1994, Stratigraphic framework of a late Pleistocene shelf-edge delta, northeast Gulf of Mexico: The American Association of Petroleum Geologists Bulletin, v. 78, p. 1276–1312.

Thomas, M.A., and Anderson, J.B., 1994, Sea-level controls on the facies architecture of the Trinity/Sabine incised-valley system, Texas continental shelf, *in* Dalrymple, R.W., Boyd, R., and Zaitlin, B.A., eds., Incised-Valley Systems: Origins and Sedimentary Sequences: Society for Sedimentary Geology (SEPM) Special Publication 51, p. 63–82.

Thornthwaite, C.W., 1948, An approach toward a rational classification of climate: Geographical Review, v. 38, no. 1, p. 55–94, doi: 10.2307/210739.

Toomey, R.S., III, Blum, M.D., and Valastro, S.V., Jr., 1993, Late Quaternary climates and environments of the Edwards Plateau, Texas: Global and Planetary Change, v. 7, p. 299–320, doi: 10.1016/0921-8181(93)90003-7.

Törnqvist, T.E., Gonzalez, J.L., Newsom, L.E., van der Borg, K., de Jong, A.F.M., and Kurnik, C.W., 2004a, Deciphering Holocene sea-level history on the US Gulf Coast: A high-resolution record from the Mississippi Delta: Geological Society of America Bulletin, v. 116, p. 1026–1039, doi: 10.1130/B2525478.1.

Törnqvist, T.E., Bick, S.J., Gonzalez, J.L., van der Borg, K., and de Jong, A.F.M., 2004b, Tracking the sea-level signature of the 8.2 ka cooling event: New constraints from the Mississippi Delta: Geophysical Research Letters, v. 31, doi: 10.1029/2004GL021429.

van de Plassche, O., 1990, Mid-Holocene sea-level change on the eastern shore of Virginia: Marine Geology, v. 91, p. 149–154, doi: 10.1016/0025-3227(90)90138-A.

van de Plassche, O., Mook, W.G., and Bloom, A.L., 1989, Submergence of coastal Connecticut 6,000–3,000 (^{14}C) years B.P.: Marine Geology, v. 86, p. 349–354, doi: 10.1016/0025-3227(89)90093-5.

Walker, K.J., Stapor, F.W., Jr., and Marquardt, W.H., 1995, Archeological evidence for a 1750–1450 B.P. higher-than-present sea level along Florida's Gulf Coast: Holocene Cycles, Sea Levels, and Sedimentation: Journal of Coastal Research, v. 17, Special Issue, p. 205–218.

White, W.A., Calnan, T.R., Morton, R.A., Kimble, R.S., Littleton, T.G., McGowen, J.H., Nance, H.S., and Schmedes, K.E., 1983, Submerged Lands of Texas, Corpus Christi Area: Sediments, Geochemistry, Benthic Macroinvertebrates, and Associated Wetlands: Austin, Texas, Bureau of Economic Geology, University of Texas at Austin, 154 p.

Wright, S.S., 1980, Seismic Stratigraphy and Depositional History of Holocene Sediments on the Central Texas Gulf Coast: Austin, Texas, University of Texas at Austin, 123 p.

Yeager, K.M., Santschi, P.H., Schindler, K.J., Andres, M.J., and Weaver, E.A., 2006, The relative importance of terrestrial versus marine sediment sources to the Nueces–Corpus Christi estuary, Texas: An isotopic approach: Estuaries and Coasts, v. 29, p. 443–454.

Manuscript Accepted by the Society 10 March 2008